5-1-2014

Hail Formation in Florida

Matthew Stanley
University of South Florida, mas3@mail.usf.edu

Hail Formation in Florida

by

Matthew Stanley

A thesis submitted in partial fulfillment
of the requirements for the degree of
Master of Science
School of Geosciences
College of Arts and Sciences
University of South Florida

Major Professor: Jennifer Collins, Ph.D.
Todd Barron, M.S.
Kamal Alsharif, Ph.D.

Date of Approval:
April 23rd, 2014

Keywords: Climate, Meteorology, Weather, Forecasting, Atmospheric Variables

Acknowledgments

I would like to thank my advisor Jennifer Collins and committee members Todd Barron and Kamal Alsharif for their input throughout the process. In addition, I would like to express my gratitude to Charlie Paxton (Science and Operations Officer, National Weather Service, Tampa Bay) and Shaza Hussein (USF undergraduate student) for their work in creating data files and graphs.

Table of Contents

List of Tables

List of Figures

Abstract

Hail poses a substantial threat to life and property in the state of Florida. These losses could be minimized through better understanding of the relationships between atmospheric variables that impact hail formation in Florida. Improving hail forecasting in Florida requires analyzing a number of meteorological parameters and synoptic data related to hail formation.

NOAA archive data was retrieved to create a database that was used to categorize text files of hail days. The text files were entered into the National Oceanic and Atmospheric Administration Earth System Research Laboratory website to create National Centers for Environmental Prediction/National Center for Atmospheric Research Reanalysis maps of atmospheric variables for Florida hail days as well as days leading to the hail event. These data were then analyzed to determine the relationship between variables that affect hail formation, in general, across different regions and seasons in Florida using Statistical Product and Service Solutions. The reasoning for the differing factors affecting hail formation between regions, seasons and hail sizes were discussed, as well as forecasting suggestions relating to region and month in Florida. The study found that the majority of all hail that occurs in Florida is during the wet season. A low Lifted Index, high Precipitable Water and lower than average Sea Level Pressure, in most cases, is present during hail days in Florida. Furthermore, results show that Vector Wind magnitude increases as hail size increases. Additionally, several atmospheric variables useful to studying hail events, such as Lifted Index, Precipitable Water, Sea Level

Pressure, Vector Wind and Temperature have significant correlations with each other depending on the region and season being observed. Strong correlations between low Lifted Index, high Precipitable Water values and the occurrence of hail events are discussed, as well as the relationship between temperature anomalies at various pressure levels and the occurrence of hail events.

Chapter One: Introduction

Florida Climate and Weather

Florida is a large and diverse state in many regards, including the state's weather and climate. Understanding this diversity is key to grasping the overall patterns of weather, including severe weather and hail events in Florida. Florida has four different Köppen–Geiger climate classifications, which is the most widely used climate classification system to classify climate types (McKnight and Hess 2000). The most extensive climate type in Florida is humid subtropical, encompassing all of North and Central Florida. The final three, located in South Florida, are all tropical climate types: equatorial savannah, equatorial rainforest and equatorial monsoon (McKnight and Hess 2000).

As described by the Köppen–Geiger climate classification, Florida has distinct wet and dry seasons. Florida's wet season runs from June to October, where precipitation is governed by sea breeze fronts and occasional tropical cyclones (McKnight and Hess 2000). Sea breeze fronts are created by strong surface temperature gradients between land and a body of water, which creates a relative low pressure on land and higher pressure at sea (at the surface) (Crosman and Horel 2010). Air flows from the high pressure toward the low pressure, causing a localized front to form at the boundary between the cool air rushing toward the warm air inland

(Crosman and Horel 2010). During the summer rainy season in Florida, rain forms at this boundary, often on a daily basis. The remaining seven months of the year (November through May) are considered the dry season (McKnight and Hess 2000). During this time, multiple baroclinic systems pass through the state bringing little precipitation. On occasion, these systems bring severe weather, and slow moving systems can bring significant precipitation (Crosman and Horel 2010).

Florida's climate is affected by the El Niño/Southern Oscillation (ENSO). During the El Niño phase of ENSO, when ocean temperatures near the coast of Peru are warmer, Florida tends to experience increased precipitation during the late autumn through the early spring months due to increased activity of the jet stream over the Southeastern United States and formation of low pressure systems in the Gulf of Mexico (Smith et al. 2007). The El Niño phase also tends to disrupt tropical cyclone development in the North Atlantic Ocean during the summer months through increased vertical windshear. The La Niña phase, on the other hand, tends to produce drier conditions during the winter with increased tropical activity in the North Atlantic Ocean due to less vertical wind shear. (Smith et al. 2007).

Florida is prone to several different severe weather phenomena. A storm is considered severe by the National Weather Service (NWS) if it meets one of three criteria: hail larger than 2.54 cm, winds exceed 25.93 m s^{-1}, or has a tornado present (a tornado warning would be issued) (National Weather Service 2013). Florida is statistically more susceptible to lightning deaths and injuries than any other U.S. state, with the highest casualties occurring in Central Florida (Hillsborough and Pinellas Counties) (Paxton et al. 2008). Florida also experiences

more tornadic activity than any other state per square kilometer (Collins et al. 2000). Tornadoes in Florida tend to form most during the summer months (many of these tornadoes form as water spouts), when mesoscale factors and the prevalence of tropical airmasses serve to challenge meteorologists daily when forecasting which thunderstorms cells may become tornadic (Collins et al. 2000). Finally, Florida experiences more tropical cyclone activity than any other state, with a hurricane striking the state every 2 years on average (Malmstadt et al. 2009). Tropical cyclones bring heavy rain, strong winds and, occasionally, tornadoes (and very rarely hail).

Hail Formation

Hailstones are irregularly shaped clumps of solid ice precipitation that may fall alongside rain during severe thunderstorms. To be classified as hail, the hailstone must be at least 5 mm in diameter according to the NWS. Storms that produce hail, known as hailstorms, pose a significant threat to economic activities, particularly agriculture and insurance companies (due to monetary loss from insurance claims) (Garcia-Ortega et al. 2001; Pflaum 1980). It is estimated that damage from hailstorms causes at least $1.2 billion in damage to property and agricultural crops each year (Basara et al. 2007).

Our understanding of why hail forms is not known with complete certainty due to the inability to observe the formation of the hailstones inside of thunderstorms. Original meteorological thought suggested that hailstones form when super cooled water droplets make contact with cloud condensation nuclei (CCN) and begin to fall through humid areas of the cloud (Pflaum 1980). Due to the "onion"-like cross-section of a hailstone, where layers of

different opacity and ice thickness are observed, theory suggested that hailstones fall through humid areas in a cloud (forming a layer around the hailstone through accretion). The hailstones are then carried upward by a strong updraft, then fall again, as seen in Figure 1, repeating the process several times to create the "onion" layered structure of the hailstone (Pflaum 1980; Nelson 1983). The hailstone will continue this process until the updraft can no longer support the mass of the stone, at which time it will precipitate to Earth in the form of hail. However, this is only partly true.

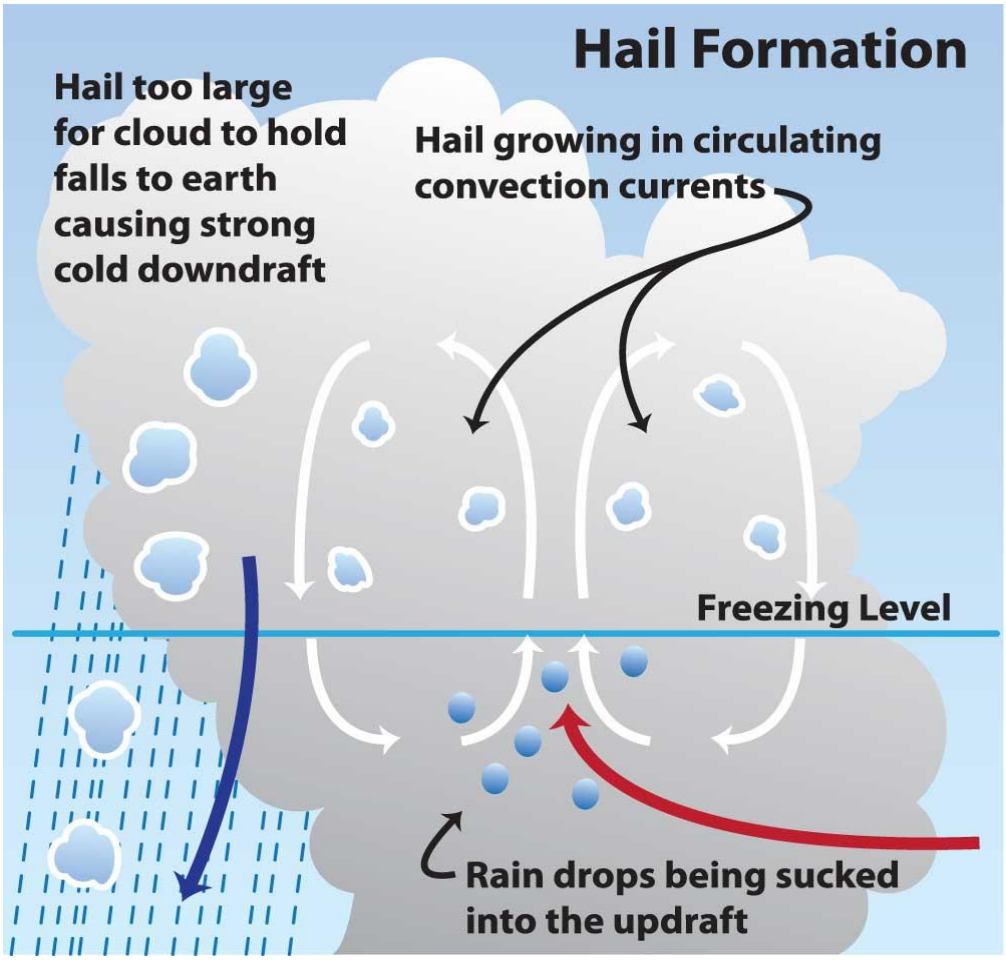

Figure 1: *Hail Formation (Scijinks 2014)*

More recent meteorological thought suggests that hail forms in the updraft of the storm.

The hailstone will grow as condensation of water (from gas to liquid) forms onto the outer surface, governed by the humidity (amount of water vapor) in the cloud (Pflaum 1980; Nelson 1983). It may also grow through accretion of super-cooled water droplets in the cloud, or even through collecting other hailstones, ice pellets or graupel (dependent on the concentration of moisture content) (Brimelow et al. 2002; Nelson 1983). While the hailstone is being driven upward by the updraft inside of a thunderstorm, it passes through various levels of humidity and moisture content (Nelson 1983). This difference in humidity and moisture content throughout the cloud is believed to be the primary reason for varying layers and irregular shapes of hailstones (Nelson 1983).

The differences between opaqueness of hailstone layers are primarily due to changes in humidity, temperature and moisture content in the cloud (Brimelow et al. 2002; Nelson 1983). When a hailstone is in an updraft that is below freezing (anywhere between -5 °C and -35 °C), but not well below freezing (colder than -40 °C), "wet growth" will occur (Brimelow et al. 2002; Farley et al. 2004; Nelson 1993). Wet growth occurs through accretion of liquid water (super cooled water droplets), where the water droplets accrete onto the surface of the hailstone and surround it in a layer. A clear or translucent layer is often the derivative of a hailstone acquiring a layer through wet growth (Pflaum 1980; Nelson 1983). "Dry growth" occurs when a hailstone travels through a layer of air with temperatures that are much below freezing (less than -40 °C), where it can only grow in size by condensation of water vapor from the surrounding humid air. White, milky, opaque layers are formed through water vapor condensing onto the hailstone in dry growth (Farley et al. 2004; Nelson 1983). These layers may appear as roughly concentric rings in a cross-section, similar to tree rings.

Differences in thickness of layers of a hailstone, however, are due mostly to the accretion rate as well as the mass (Nelson 1983). The accretion rate is largely dependent on the time spent in an area of relatively uniform humidity or uniform moisture content; the longer the hailstone and moisture coincide, the thicker the layer can become. The time a hailstone and such a moisture source are together depends largely on the velocity of both the hailstone and the super cooled water droplets (or only the former if accretion through dry growth is occurring) (Nelson 1983). The result of this is that layer thickness (and the accretion rate) is largest when a hailstone is caught in a weaker part of an updraft, where it will be slower than if it were in the strongest part of the updraft (Nelson 1983). If the hailstone were in a weaker part of the updraft moving upward more slowly, it would have more time to gain layer thickness through accretion as opposed to a hailstone in the highest velocity section of the updraft. Recent hail growth modeling supports this, as one study found the largest hailstones, and most hail growth, occurring in a narrow region within a weak updraft zone (Farley et al. 2004). In addition, the slower the downward velocity of super cooled water droplets (spending more time near the hailstone), and the higher the mass of the hailstone (a more massive hailstone has a lower upward velocity), the thicker the layers of a hailstone should be due to increased accretion (Nelson 1983).

Finally, most hailstones primarily form at a density near 0.9 g cm^{-3} (Brimelow et al. 2002). This type of hail forms most often in thunderstorm clouds through both wet growth and dry growth when liquid water content is high and/or updrafts are strong (Pflaum 1980). This accounts for the majority of hail that forms, but another kind of hail, low density hail, can form

in different conditions (and may not always be accounted for). Low–density hail can form in areas of low temperatures, low moisture content and weak updrafts in a thunderstorm cloud (much like graupel) (Brimelow et al. 2002; Pflaum 1980). This type of hail forms like graupel, where a hailstone will accrete porous (low-density) ice to the surface of the stone (a process known as riming) (Pflaum 1980).

Causes of Hail

Meteorologists have come to understand many of the factors and variables involved in setting up an environment, synoptic pattern and mesoscale pattern conducive for the formation of hail. The most obvious prerequisite to hail formation is the presence of a thunderstorm (Kaltenböcka et al. 2009; Longley and Thompson 1965; Sanchez et al. 2003). Hailstones form only within a strong convective cell but can also fall outside of the cell (within 3.7 km). Severe thunderstorms are storms that produce hail over 2.54 cm, produce winds at or above 26 m s^{-1} and/or contain funnel clouds or tornadoes as described by the NWS (National Weather Service 2013). The thunderstorm cells in which they form tend to be associated with baroclinic systems (most often cold fronts) in organized bands of thunderstorms known as mesoscale convective systems (Longley and Thompson 1965; Sanchez et al. 2003). Within these thunderstorms, hailstones form and grow most often in the "forward flank" region (area of highest precipitation), near the boundary of the primary updraft and the forward flank downdraft (Farley et al. 2004).

One of the primary factors identified for the environment to be conducive for hail development is the presence of relatively warm air in the atmosphere (Longley and Thompson

1965). It is estimated that an ideal temperature of about -1°C at 700 hPa is favorable for the formation of hail (just below freezing) (Longley and Thompson 1965). Warm temperatures should extend in a column from near the surface into the middle troposphere, with much cooler temperatures outside of the column (Aran et al. 2007). This allows for both the formation of frozen precipitation (the hailstone) and the presence of liquid moisture (in the form of super cooled water droplets) conducive for the growth of a hailstone. Temperatures that are too cold hinder the development of most types of hail and limit wet growth (Longley and Thompson 1965).

Another synoptic factor that contributes to the formation of hail is the presence of positive vorticity advection (Longley and Thompson 1965). Vorticity simply is a measure of the rotation or spin in the atmosphere. It is known that positive vorticity advection often is associated with instability and is used extensively in forecasting super cell thunderstorms, which tend to be accompanied with hail. In a case study focused on Alberta, Canada, it was noted that positive vorticity advection was related to a trough on days with major hail events (and to a lesser extent, minor hail events) (Longley and Thompson 1965).

Some other major variables used by meteorologists to identify conditions for the formation of hail include mean sea level pressure (MSLP) and geopotential height (Aran et al. 2007). Low MSLP may indicate instability. When the pressure is low at a given point, there is less mass above that point compared to surrounding points at the same altitude. This causes air to rush to the low-pressure area, which once it converges, causes air to be pushed vertically, creating an updraft. Updrafts are a key ingredient to thunderstorm activity and hailstone

formation; therefore measuring MSLP is valuable when looking at conditions conducive to hail formation at the synoptic scale (Aran et al. 2007). Geopotential height is a measure of the altitude above the surface at a given pressure level. Lower geopotential height can be associated with areas of lower MSLP. If a geopotential height in one location were lower than surrounding locations at a particular pressure level(s) (say, 900 hPa, 850 hPa and 700 hPa), this would indicate an area of low height, and therefore low pressure, at that specific point above the surface. Low pressure is conducive for the formation of thunderstorms, which leads to hail formation.

A major variable in measuring instability, convective available potential energy (CAPE), can also be used to determine areas of likely hail formation (López et al. 2001). CAPE is a measure of buoyant energy between the level of free convection (LFC) and the equilibrium level (Sánchez et al. 2003). High values of CAPE have been correlated with the formation of hailstorms within severe thunderstorm complexes (López et al. 2001). It has been suggested that measuring various CAPE indices may help to identify areas prone to hailstorms (Sánchez et al. 2003). Since high CAPE values have been associated with the development of severe thunderstorms (López et al. 2001), a higher CAPE index can be one potential indicator of stronger thunderstorms and hail formations.

Another widely used index when measuring instability is the Lifted Index (LI). To obtain the Lifted Index value, one must theoretically take an air parcel and lift it, adiabatically (no heat input or output), to a given pressure height (most commonly 500hPa) (DeRubertis 2006). Then, the difference between the temperature of the air parcel and the temperature of the

environment around the air parcel is the value of the Lifted Index (DeRubertis 2006). A positive value for the Lifted index represents a stable atmosphere (the higher the positive number, the more stable), while a negative number represents an unstable atmosphere (the more negative the number becomes, the less stable the atmosphere) (DeRubertis 2006). While indices such as CAPE are considered more reliable, there are still many studies on severe weather and hail that use the Lifted Index. Studies have found that Lifted Index correlated best with hail measurements using hailpad hits (Manzato 2003). Lifted Index has been used successfully in other studies focusing on hailstone size (Palencia et al. 2012) and correlations between severe weather indices and hail events (Manzato 2012).

Another variable in identifying areas susceptible to hailstorms is vertical wind shear (Sánchez et al. 2003). Vertical wind shear is a combination of both the change of wind direction and the change of wind speed with height. When the wind shear value is large (large changes in wind direction and wind speed with height) in an unstable environment, thunderstorms tend to produce strong, long-lived thunderstorm complexes (Sánchez et al. 2003). However, weak wind shear is not conducive for development of strong storm complexes, and is instead indicative of a small, short-lived thunderstorm cell (Sánchez et al. 2003). Since both CAPE and vertical wind shear play roles in the strength of thunderstorms (and therefore the likelihood of hail development), the Bulk Richardson Number was developed to combine these values. The Bulk Richardson Number is simply the ratio between CAPE (which measures instability) and wind shear vector difference (Sánchez et al. 2003). The Bulk Richardson Number can be related to situations favoring super-cell and multi-cell thunderstorm development (often accompanied with hail) (Sánchez et al. 2003).

Hail Forecasting and Observation

Hailstorms are difficult to predict (López et al. 2005). There are two primary reasons for this: the relatively small area that hailstones actually fall during a thunderstorm and the short duration of hail events (López et al. 2005). However, through understanding variables that affect hail development, synoptic scale patterns, and the microphysics of hail formation (discussed in the previous two sections), forecasting strategies and models can, to a certain degree of accuracy, determine the likelihood of a hail event. Current forecasts for the likelihood of hail by the NWS extend out to only a few days, and cover large (hundreds of square kilometers) of area, while more precise hail prediction tends to be only minutes in advance (when a severe thunderstorm warning is issued that details accompanying hail) (López et al. 2005; Garcia-Ortega et al. 2001). Giving more advanced warning and precision in hail forecasts will undoubtedly prevent some of the economic loss associated with hailstorms (Garcia-Ortega et al. 2001).

Hail forecasting is done primarily through various dynamical and statistical models used to predict day-to-day weather, such as the Global Forecast System (GFS), the European Centre for Medium-Range Weather Forecasts (ECMWF), and others. Models are used not only to predict where hail will occur, but numerical models, such as the GFS and ECMWF, can also estimate the size of hail that will precipitate to the ground with marginal success (Brimelow and Reuter 2009; Kaltenböcka et al. 2009). However, improving upon these models is possible and has been done in many case studies. In one case study, López et al. (2005), taking into account

many of the variables discussed in the previous section, created a forecast model for hail events specific to Spain. The model included variables identified as crucial to the formation of hail, including, but not limited to, temperature (at various levels of the atmosphere), pressure (at various levels), dew point temperature (at various levels), relative humidity (at the surface), LFC, the lifting condensation level (LCL), convective temperature, the height of the 0°C isotherm, and wind speeds and directions at various heights (López et al. 2005). Accounting for all of these in a model, as well as topographical features and synoptic patterns specific to the region of study, the model produced a probability of detection of .867 and a false alarm rate of only .187 (López et al. 2005).

Other case studies focus more on stability indices. For example, one case study examined various stability indices identified by past literature, as well as CAPE, vertical wind shear intensity and the Bulk Richardson Number (Sánchez et al. 2003). While the model found success in identifying mesoscale systems and complexes (areas of organized storm activity which often produce hail), the study produced only moderate success in identifying hail-producing storms. This suggests the need to incorporate more variables or to increase spatial and temporal frequency of soundings that record data used to valuate indices such as CAPE (Sánchez et al. 2003).

Perhaps one of the more successful models came from the use of a multivariate scheme. In this case study, classifications were made for 260 hail days in the middle Ebro Valley of Spain using National Center for Environmental Prediction (NCEP)/National Center for Atmospheric Research (NCAR) Reanalysis (2.5° x 2.5°) data to characterize synoptic

conditions during the hail days (Sánchez et al. 2003; Kalnay et al. 1996). The five variables considered from this NCEP/NCAR reanalysis were temperature at 500 hPa, temperature at 850 hPa, pressure at 500 hPa, pressure at 850 hPa and relative humidity at 850 hPa. A Principal Component Analysis (PCA) was conducted followed by a Cluster Analysis (CA) (Sánchez et al. 2003). The PCA is used to reduce the amount of data put into the model as well as ensure that only the principal variation modes of the 260 hail days are used for the CA (in this multivariate scheme, at least 90% of the total variance is accounted for) (Sánchez et al. 2003). After the PCA was applied and components stored for each of the five variables, the CA was applied to create interpretable results, separating the hail days into 5 "clusters" defined by different characteristics (Sánchez et al. 2003). The characteristics of each cluster, upon examination, can be used by forecasters in the Middle Ebro Valley to observe synoptic conditions that lead to hail formation, For example, Cluster #1 hail days occur mostly in May and September when an unusually strong low forms south or southwest of the Iberian Peninsula (Sánchez et al. 2003).

Satellite imagery of infrared sensors is used to show cloud-top temperatures of thunderstorms to indicate areas where strong thunderstorms are located (Heinselman and Ryzhkov 2006). Radar data are primarily used as a basis for hail warnings. First-hand accounts of hail sightings are used to confirm hail forecasts and warnings. First-hand accounts can now easily be uploaded and verified via social media outlets such as Facebook and Flickr (Cecil and Blankenship 2012; Heinselman and Ryzhkov 2006; Hyvärinen and Saltikoff 2010). Traditional radars (single polarization) have been used to detect hail by using single-radar reflectivity. The use of traditional radar systems, however, is at a disadvantage compared to newer polarimetric radars. The trajectory, shape and motion of hailstones within a cloud are much more random

than raindrops (Heinselman and Ryzhkov 2006). Polarimetric radars can better measure shapes and orientations of hailstones and raindrops, allowing for a better technique in identifying hailstones (Heinselman and Ryzhkov 2006).

Hail, Climate Modeling and the Future

Future hail events will be affected by the progression of climate change (Cecil and Blankenship 2012; Leslie et al. 2008). One study used climate simulations in Australia to estimate future climate scenarios if greenhouse gases (GHGs) were kept at present levels and if they were to rise as expected (Leslie et al. 2008). The University of Oklahoma Coupled Global Climate Model was used. This is a high-resolution (1km resolution with 40 vertical levels) mesoscale model. A strong correlation was found between the increase in GHGs in the atmosphere over the 50-year period and the number of severe hailstorms (Leslie et al. 2008).

With such possible trends, it will be important to build up future climatologies of hail events. Cecil and Blankenship (2012) created an 8-year climatology, using microwave scanning over the entire globe. The satellite data generally lined up with actually recorded events, finding that the most severe hail in the United States occurs in the Deep South and Plains regions (Cecil and Blankenship 2012). In Florida, there were multiple large hail reports (over 2.5cm as defined by the NWS) over this 8-year period (Cecil and Blankenship 2012). Looking to the future, model simulations (similar to those in Leslie et al. 2008) combined with creating climatologies of regions (as studied in Cecil and Blankenship 2012) may be influential to other studies when addressing the question of how hail is affected by climate change.

Problem Statement

Multiple problems are noted regarding hail and forecasting. Hail can be a danger to life and property, and may continue to worsen as effects from climate change continue to manifest (Basara et al. 2007; Leslie et al. 2008). However, modeling and forecasting is not yet as accurate as some would like it to be (Garcia-Ortega et al. 2001; Pflaum 1980). Hail forecasting is difficult because hail often occurs in a small scale over a short duration, but needs to be improved to become more precise and accurate on a local and regional scale (López et al. 2005; Garcia-Ortega et. al. 2001). The public also continues to be misled by false alarms of hail events, which can be reduced (López et al. 2005). The goal of this study is to address these issues by understanding variables that affect hail formation, specifically in Florida, that may lead to better hail forecasting methods on a regional and seasonal scale.

Objectives and Research Questions

After reviewing literature and formulating ideas about studying hail events in Florida, a few basic themes are apparent. First, the literature involving the different variables which lead to hail formation (Brimelow et al. 2002; Nelson 1983; Sánchez et al. 2003; Derubertis 2006) is well studied, but more could be done to determine which are most important in the formation of hail. For example, how strongly correlated are lower Lifted Index values and the occurrence of hail (and hail size)? Second, the literature defining the importance of focusing on a regional scale most influenced preparation for the research (Sánchez et al. 2003; Brimelow and Reuter

2009; Kaltenböcka et al. 2009). These studies focused on collecting and using data specific to a region (a United States' state, a province within a country, etc.) to determine which atmospheric variables were most important in forecasting for hail events in those regions. For example, hail events in the Great Plains region of the United States may be more easily predicted by a lower Lifted Index value than a hail event in Florida.

The objectives and questions below reflect on these two thoughts and most influenced preparation for the research.

Objectives:

1. To create a better understanding of the atmospheric variables which impact hail formation and hail events in Florida through use of the National Oceanic and Atmospheric Administration (NOAA) National Climate Data Center (NCDC) storm event database and NCEP/NCAR Reanalysis data of days of hail events and days leading up to hail events.

2. To use the knowledge of atmospheric variables for each specific region, month grouping and hail size distribution to determine which factors are most critical for the formation of hail in different regions of Florida through various seasons.

3. To suggest better hail forecast methods and extend hail forecast range for Florida, based on a regional and/or seasonal scale, incorporating results from objectives 1 and 2.

Research Questions:

1. Which atmospheric variables are most important for forecasting hail events in different regions of Florida and which atmospheric variables indicate the potential for hail events in Florida days prior to the event?

2. How do atmospheric variables vary between hail events and hail size?

3. How do hail days differ between months and seasons and what are the seasonal differences of the atmospheric variables?

4. Are the mean month and mean seasonal climatological differences significant enough to warrant a regional hail forecast system or to change the way hail is forecast in Florida?

Chapter Two: Research Methodology

Study Area and Data Collection

The NOAA NCDC online storm event database, found at http://www.ncdc.noaa.gov/stormevents/, was used to identify hail days in Florida between 1950−2010, since when NOAA began first recording hail events (NOAA does not keep records of "hail" less than .5" in diameter, as this is not considered hail) (National Weather Service 2013). In this time period, there were a recorded 4025 total hail events in the state of Florida. Regionally, 497 hail events occurred in Northwest Florida (Figure 2), 1090 hail events occurred in Northeast Florida, 1888 hail events occurred in Central Florida, and 523 hail events were recorded in South Florida. The objective of collecting these data was twofold: to analyze where hail occurs in Florida and where the largest hail falls to gain an initial understanding of hail patterns and to analyze specific atmospheric variables using NCEP/NCAR Reanalysis (Kalnay et al. 1996) (similar to the work of Garcia-Ortega et al. 2011) for all hail days in Florida. The NCEP/NCAR Reanalysis is an analysis and forecasting system used for data assimilation, and is able to retrieve data from 1948 to the present. Using the NOAA/NCDC data, a spreadsheet database was created to organize the data by hail size distribution (<1.00", 1.00", 1.25-1.75", 2.00", 2.25-2.75", 3.00", 3.25-3.75", 4.00", 4.25-4.75" in diameter), average hail size by month, and largest hail size by month.

There were a total of 781 hail days with less than 1.00” hail, 464 hail days at 1.00”, 537 days from 1.25-1.75”, 54 hail days with 2.00” hail, 30 hail days from 2.25-2.75”, 3 days of 3.00” hail, 1 day of 3.25-3.75” hail, 1 day of 4.00” hail and 2 days of 4.25-4.75” hail; for a total of 1873 total hail days (compared to the total of 4025 hail events in Florida).

Text files were created from each hail size, within each month grouping (Feb-May, Jun-Sep, and Oct-Jan). This resulted in 15 files for Northwest Florida, 15 files for Northeast Florida, 13 files for Central Florida, and 13 files for South Florida (these would later be used as the “n” values in the Pearson Correlation). Files were later created for month groupings as well, resulting in 25 text files for the Feb-May grouping, 18 files for the Jun-Sep grouping, and 13 files for the Oct-Jan groupings (used only in the Pearson Correlation later). All four regional text files were uploaded to the NOAA Earth System Research Laboratory (ESRL) website and used to create NCEP/NCAR Reanalysis images.

The next step was to organize a hail file using the raw data taken from the NOAA archive data. Within each region, spreadsheets were created to separate the total number of hail occurrences per month and the largest hail recorded for each month, resulting in four spreadsheets (one for Northwest, Northeast, Central and South Florida). These spreadsheets were used to create graphs comparing the number of hail occurrences per month vs. the largest hail size per month.

The hail file consists of text files (.txt) that were imported into the NOAA ESRL website and split into 4 subcategories based on geography, and categorized further after that (Figure 2).

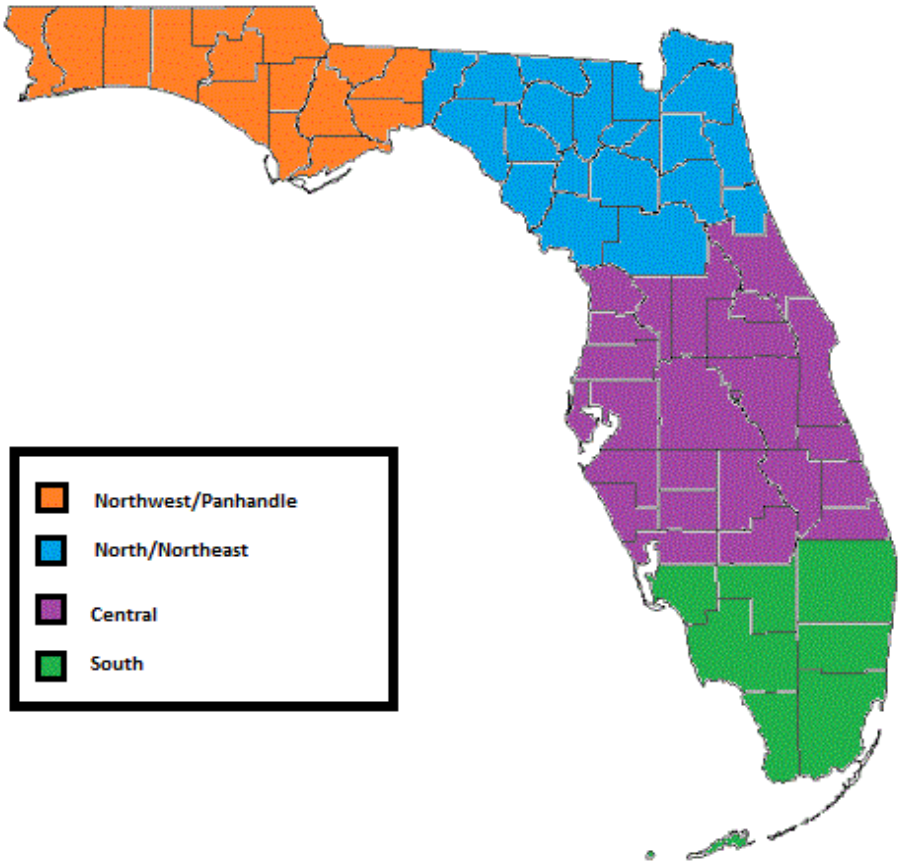

Figure 2: *County shapes map retrieved from http://www.myonlinemaps.com/florida-county-map.php. (Retrieved 10 Jan 2013)*

The first region is Northwest Florida along the coastal Florida Panhandle encompassing the counties of: Escambia, Santa Rosa, Washington, Okaloosa, Holmes, Walton, Bay, Jackson, Calhoun, Gulf, Franklin, Liberty, Gadsden, Leon and Wakulla. The second region consists of North and Northeast Florida, with a climate type similar to the Panhandle but includes many more inland areas, encompassing the following counties: Jefferson, Madison, Taylor, Hamilton, Suwannee, Lafayette, Gilchrist, Dixie, Levy, Marion, Alachua, Union, Columbia, Baker, Nassau, Duval, Bradford, Clay, St. John's, Putnam and Flagler. The third region covers the area

of the Central Florida Peninsula, where regular sea breeze fronts from both the east and west coast of the state play a large role in day-to-day weather throughout a large part the year (Case et al. 2005). The Central Florida Peninsula included: Citrus, Hernando, Pasco, Pinellas, Hillsborough, Manatee, Sarasota, Charlotte, Glades, Desoto, Hardee, Highlands, Polk, Sumter, Lake, Volusia, Seminole, Orange, Osceola, Okeechobee, Martin, St. Lucie, Indian River and Brevard Counties. The final region encompasses the remaining Florida counties in South Florida, which is perhaps the most distinct region based on climate types (McKnight and Hess 2000): Lee, Collier, Monroe, Hendry, Palm Beach, Broward and Miami-Dade.

Within these four geographic subcategories, three different month groupings were created within each geographic region. The month groupings are February-May, June-September, and October-January based on Florida climatology outlined in McKnight and Hess (2000). The dry season was split into fall/winter and spring groupings. Finally, the last subcategories within the month groupings were a hail size grouping. These groupings were taken from the spreadsheet database previously created (<1.00", 1.00", 1.25-1.75", 2.00", etc.), with only the largest hail size on each day (also taken from the created spreadsheet) used. For example, if the largest hailstone recorded in Leon County, FL on 1 January 2010 was 1.12", then this date would be filed under Northwest Florida/Panhandle, October-January, 1.00" (due to rounding).

NCEP/NCAR Reanalysis composite images were obtained from the ESRL website. These images average the conditions of each date within the date file, creating a composite image for any variable selected. For example, if 55 <1.00" hail days occurred in Northwest

Florida between February and May, the 55 dates would be uploaded and the weather conditions, such as surface temperature, would be averaged and output in an image.

This process was repeated for every region, month grouping and hail size distribution for a variety of variables. The variables chosen from the NCEP/NCAR Reanalysis images were based primarily on the literature (Longley and Thompson 1965; Derubertis 2006; Aran et al. 2007):

Air Temperature: 850hPa, 600hPa, 500hPa, 400hPa (anomaly) (Celsius)

Vector Wind: Surface, 925hPa, 850hPa, 700hPa, 500hPa, 300hPa, 200hPa (mean) ($m\ s^{-1}$)

Precipitable Water: Surface (mean) ($kg\ m^{-2}$)

Lifted Index: Surface (mean) (an index, no unit)

Sea Level Pressure: Surface (anomaly) (hPa)

Vector wind can be used to observe overall synoptic patterns (troughs, ridges, etc.) in the days leading up to a hail event and the day of the hail event, as well as used in the statistical analysis to compare different atmospheric variables. Precipitable Water is a measurement of the amount of moisture content in the atmosphere (if all water were to rain to the surface). Air temperature, Lifted Index and Sea Level Pressure were all chosen due to their extensive discussion in the literature and use in studies (Longley and Thompson 1965; Derubertis 2006; Aran et al. 2007).

Methodology of Objectives

Objective 1

"*To create a better understanding of the atmospheric variables which impact hail formation and hail events in Florida through use of the National Oceanic and Atmospheric Administration (NOAA) National Climate Data Center (NCDC) storm event database and NCEP/NCAR Reanalysis data of days of hail events and days leading up to hail events."*

To create an understanding of some of the atmospheric variables that impact hail events in Florida, values of the variables were recorded and put into a spreadsheet for each date file. The values of each variable were recorded from the NCEP/NCAR Reanalysis composite maps for each date, region and hail size. For example, if the air temperature at 850hPa is 26 °C according to the NCEP/NCAR Reanalysis composite data (for a specific date file), then this value was recorded in the spreadsheet.

A more subjective analysis was conducted from synoptic meteorological literature. For example, Lifted Index values play a role in forecasting the occurrence of severe weather, including hail (DeRubertis 2006). By analyzing NCEP/NCAR Reanalysis composite maps of Lifted Index values across the United States up to 3 days before a hail event occurs in Florida, a pattern was observed that links Lifted Index values, several days prior to a hail event in Florida to a hail event.

Objective 2

"To use the knowledge of atmospheric variables for each specific region, month grouping and hail size distribution to determine which factors are most critical for the formation of hail in different regions of Florida through various seasons."

The spreadsheet created from objective 1, containing values of the variables for hail days in different regions of Florida, was used for objective 2 to create correlation coefficients. A correlation coefficient (using Statistical Product and Service Solution (SPSS) software) was obtained to determine whether or not a specific variable is correlated with the occurrence of hail. For example, it could be determined if temperatures at 850hPa are correlated with other variables, such as temperature at 500hPa, on a hail day in Florida through obtaining a correlation coefficient. A correlation test using the Pearson method was used to determine a correlation coefficient for each variable pairing. It may be determined, for example, that variables are correlated in one region of Florida, in one month grouping, or one hail size distribution, but not another. The confidence of the correlation coefficient was measured by a test of significance. Nearly all results discussed in later sections are significant at least to the 5% level.

Objective 3

"To suggest better hail forecast methods and extend hail forecast range for Florida, based on a regional and/or seasonal scale, incorporating results from objectives 1 and 2. "

From the statistical data (correlation coefficients), suggestions for better forecasting methods can be made. It may be the case that, for example, high valued vector wind means at certain heights are more positively correlated with hail events in Northwest Florida/Panhandle than in South Florida. This would be valuable information for forecasting hail events for both Northwest Florida, where high valued vector wind means could indicate a higher chance of hail (and can be reflected in the forecast), as well as South Florida, where false alarm rates may be reduced by not putting as much weight into high valued vector wind means. Some variables may also be more correlated with hail events based on the month groupings (roughly, seasons), similar to how they differ between regions.

Analyzing the patterns of variables, such as vector wind mean or Lifted Index, may show synoptic patterns over regions of the United States that indicate a future hail threat as far as 3 days. But extending the forecast range may require more subjective methods, as described in objective 1. Using synoptic meteorological knowledge and the NCEP/NCAR Reanalysis data collected, it may be possible to extend hail threat notices beyond the normal few days currently given to the public.

Chapter Three: Results and Analysis

Size of Largest Hail vs. Number of Hail Occurrences

The Northwest Florida region is summarized in Figure 3. The graph shows the strong correlation between number of hail events in each month and the occurrence of large hail size in the late winter months through the early summer (February-July). The smallest hail sizes, as well as a smaller number of hail days, occurs mostly in the fall and early winter months (September-January).

The relationship of more hail days and larger hail sizes in the months from February-July can be explained by typical Florida seasonal patterns. The spring months bring baroclinic forcing through the region with arrival of cold fronts (shifting of jet streams), causing the potential for severe storms (which may bring hail). During the summer months in the Northwest Florida Region, thunderstorms develop through sea-breeze fronts, occasional cold or warm fronts, and rarely, hail from a tropical cyclone.

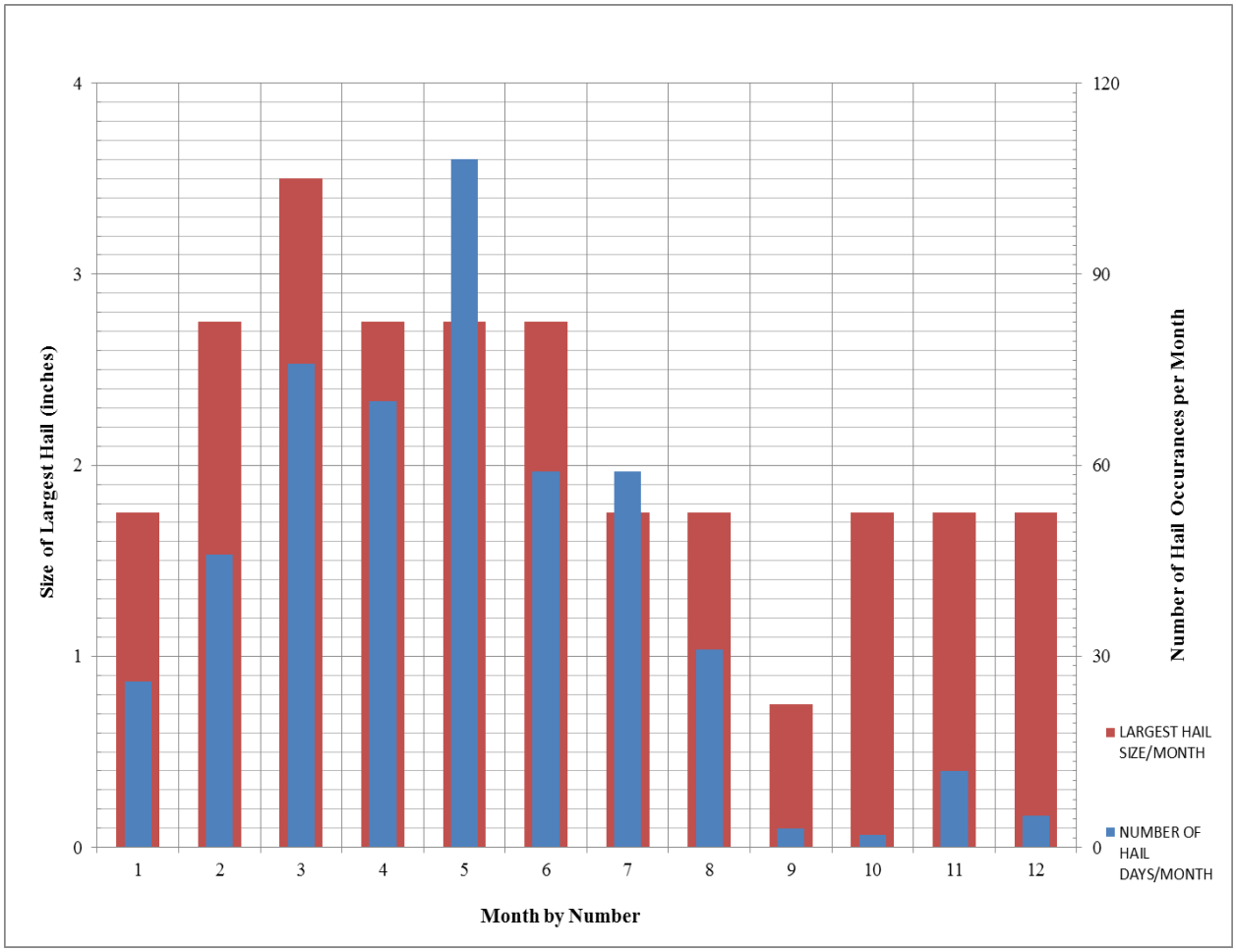

Figure 3: *Northwest Florida: Size of Largest Hail vs. Number of Hail Occurrences per Month (Over Study Period 1950−2010)*

The Northeast Florida region is summarized in Figure 4. This region is comparable to the Northwest region, where the spring and early summer months have the most hail occurrences and the largest hail sizes. It is worth noting that this region has the record for largest hail size recorded in all of the state of Florida, with 4.5” readings in both March and May. The Northeast area, with larger hail in the spring, has fronts and sea breeze weather in the summer which help create enough instability for thunderstorms and hail.

The only notable difference between Northeast and Northwest Florida comes in the months of January and February, where hail has occurred more often with larger hail sizes in the Northwest than the Northeast. This may be explained by a difference in the strength of frontal systems that reach the Northwest region and Northeast region of Florida in the winter months.

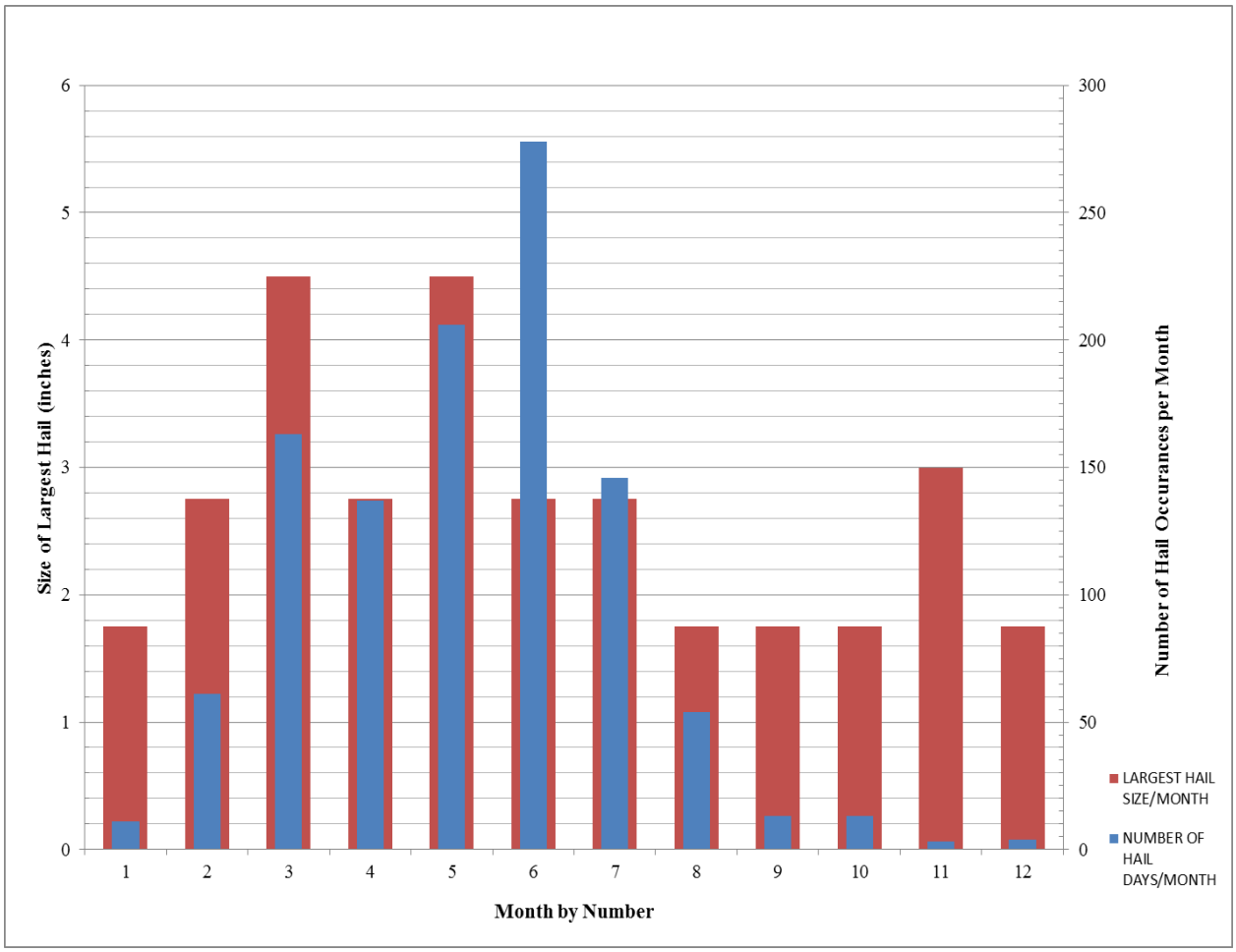

Figure 4: *Northeast Florida: Largest Hail Size vs. Number of Hail Occurrences per Month (Over Study Period 1950−2010)*

Figure 5 shows that winter and late summer month hail size and occurrence is more similar to those in Northeast Florida than Northwest Florida. However, in Central Florida, a

contrast is seen between the largest hail size occurrences and the number of hail days per month. The number of hail days per month is substantially larger in the summer months (May-July) than in the late spring (March and April). However, the largest hail occurs in March, which has almost half the number of hail days as May and June.

The difference in the number of hail days can be explained by the common clash of two sea-breeze fronts (one from the Gulf of Mexico and one from the Atlantic Ocean) over Central Florida during the summer months, which often results in thunderstorms severe enough to form hailstones. However, these storms are not usually as severe as late winter and early spring storms brought by cold fronts. The passage of cold fronts is not as common as the collision of the two sea-breeze fronts, resulting in a lower number of overall hail days in the late winter and early spring, but larger hail sizes (see Figure 5).

Figure 6 illustrates the similarity between hail occurrence and severe hail that the South Florida region shares with Central Florida as compared to Northwest and Northeast Florida. The major difference between the two regions is that Central Florida has far more hail occurrences overall than South Florida, which may be primarily from the geographic area that is designated as “South Florida” in Figure 2, (it is clear Central Florida covers a much larger area than South Florida, attributing to the much larger number of hail days in the former region). Another factor for South Florida having the least number of overall hail days compared to other regions may be that cold fronts do not reach South Florida as often as the other regions due to latitude and differing climate types (see Figure 6).

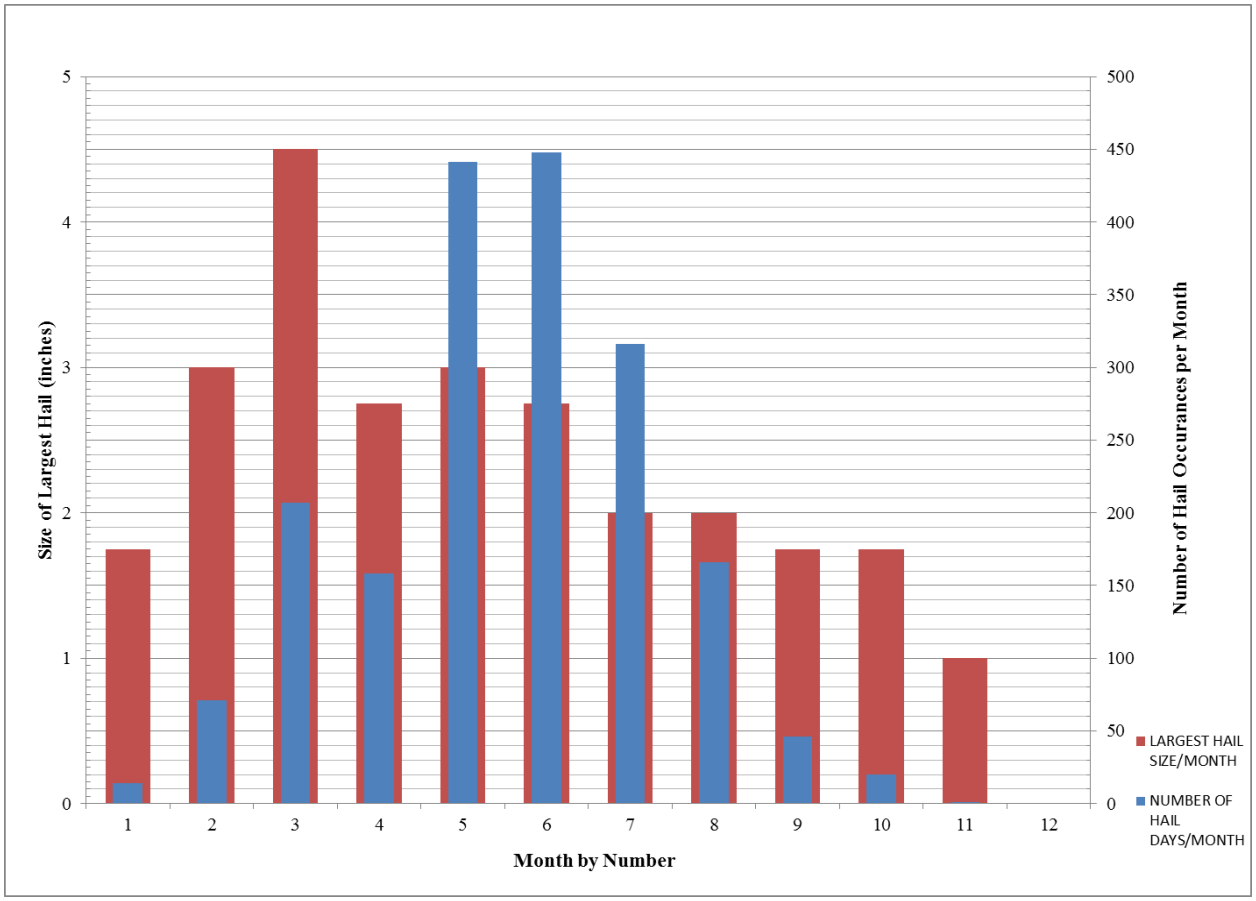

Figure 5: *Central Florida: Largest Hail Size vs. Number of Hail Occurrences per Month (Over Study Period 1950−2010)*

Text Files and NCEP/NCAR Reanalysis Images

Hundreds of NCEP/NCAR Reanalysis composite images were created to represent the average conditions (such as Lifted Index, Precipitable Water, Sea Level Pressure, Temperature at various heights and Vector Wind at various heights) for hail days within each geographic area, within each month grouping and within each hail size. Additionally, images for the average conditions for the three days prior to each hail composite were harvested, for a total of 56 images per file. For example:

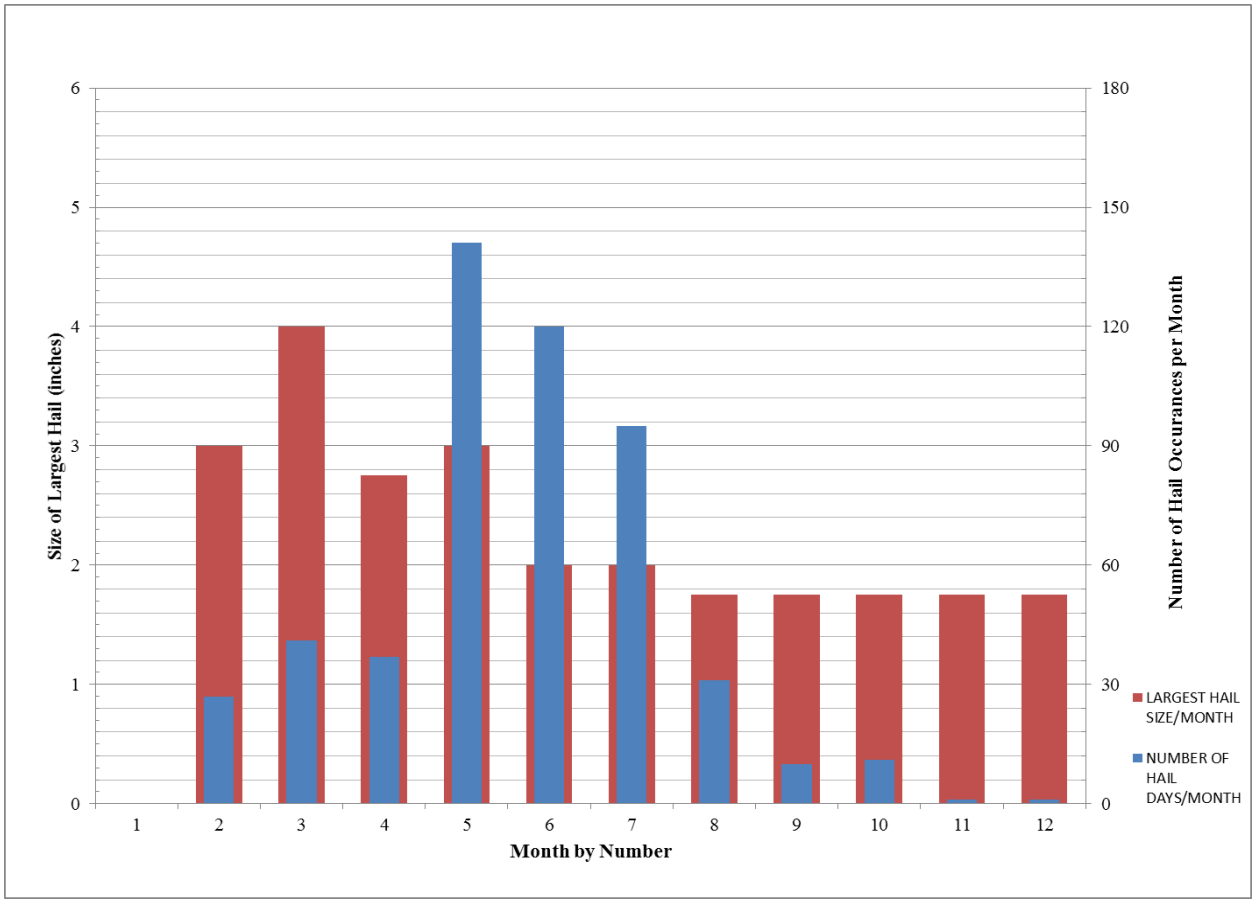

Figure 6: *South Florida: Largest Hail Size vs. Number of Hail Occurrences per Month (Over Study Period 1950−2010)*

Figure 7 is a composite of the Lifted Index value of 41 hail days that occurred between June and September (over the study period from 1950−2010) in South Florida with a maximum of 1" hail size. This image shows that the average Lifted Index value for the South Florida region is below -4, but higher than -5, yielding an average Lifted Index of -4.5 for the region. This was also repeated for the conditions for three days prior (day -1, day -2, day-3) and for each variable. Values for every image/variable were assigned by viewing the NCEP/NCAR Reanalysis images for values as just stated; by viewing the isolines on each image to determine the average conditions over a region.

The assigned values for each image were placed into spreadsheets, one for each file. This was done to compare the values of variables between regions, month groupings and hail sizes. However, to more accurately compare the differences between the different atmospheric variables with respect to hail inch size, the assigned values needed to be weighted according to the number of hail days present in each file. An equation was created for each hail inch category to properly weight each file according to the number of hail days in each file. For example, the file consisting of all hail days for the Northwest region of Florida from October-January for 1" hail numbers only 6 days, compared to the file consisting of all Central Florida hail days between June and September that were 1", which numbers 123 total days.

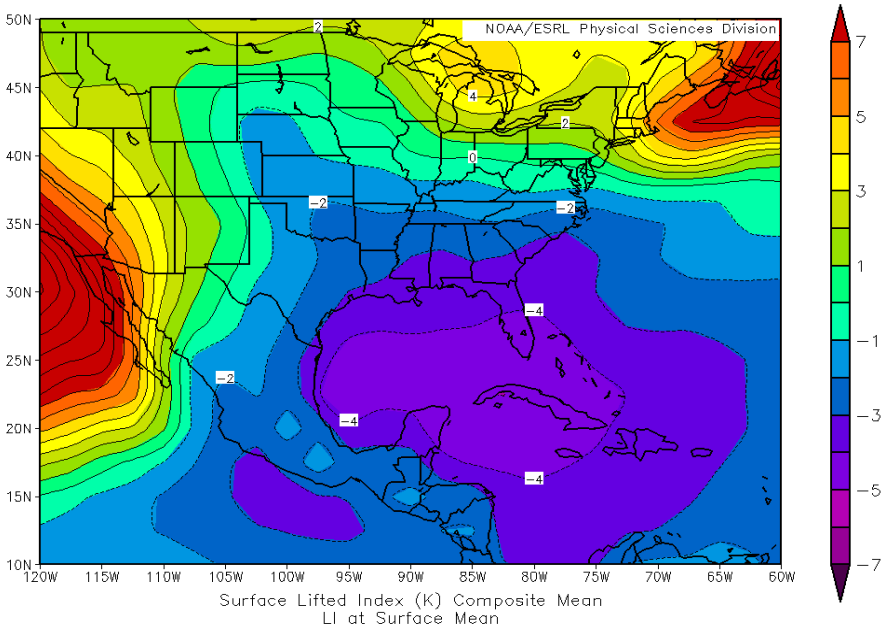

Figure 7: *Lifted Index Mean, at the Surface (day 0). Retrieved January 10 2013(Kalnay et al. 1996)*

Analysis of Hail Size Variable Weighted Averages

Table 1 details the Weighted Lifted Index Values of hail days, arranged according to hail size (far left column). The second column is the Weighted Lifted Index Value for the days of the hail events (day 0), the third column shows the Weighted Lifted Index Value for the days prior to the hail events (day -1), continuing the same pattern for the fourth (day -2) and fifth (day -3) columns. This format is used for each variable following this. This arrangement allows for analysis of not only the weighted variables with respect to hail size, but also for analysis and comparison of the weighted variables between day 0, day -1, day -2 and day -3.

For the Weighted Lifted Index, there was little variation in the average Lifted Index between the various hail sizes. Interestingly, the average Lifted Index, overall, rose between <1" to 2.25-2.75" (with the exception of the 2" category). The two values given for the 2.25-2.75" category on day 0 represent the average value of the Lifted Index with all data (-1.669) and without one extreme, possible outlier in that specific file (-2.147). One should note that for the larger hail sizes (3+) the sample size is very small (as low as n=1), therefore the average Lifted Index values listed may not be a perfect or accurate representation of "textbook" conditions for hail to form.

On the other hand, there is a clear increase in the average Lifted Index during the days prior (day -1, day -2, day -3) compared to the average Lifted Index on day 0; with the Lifted Index value increasing each day back, with the exception of the third day in some cases. The rise in the weighted average Lifted Index seems to taper off or even reverse (as just stated) by

day -3. Recall that Lifted Index is a way to quantify instability in the atmosphere, so lower values would be expected on day 0 (day of the hail event), as thunderstorms, and consequently hail, tends to form in a more unstable environment (DeRubertis 2006).

Table 1: Lifted Index (LI, Average) at Various Hail Sizes (Day 0,-1,-2,-3)

Size (inches)	LI, 0	LI, -1	LI, -2	LI, -3
<1	-3.162	-2.294	-1.62	-1.415
1	-3.021	-2.104	-1.188	-0.944
1.25-1.75	-2.887	-1.529	-0.803	-0.51
2	-3.091	-1.512	-0.296	-0.178
2.25-2.75	-1.669 / -2.147*	0.101	1.76	2.482
3	-0.67	4.85	5	2.47
3.25-3.75	-3.5	-2	8	13
4	-4	-3	-1	0
4.25-4.75	3	4	4	5

**If one extreme, possible outlier were removed from the list of hail days for this file*

Precipitable Water (PW), in Table 2, is a way to measure the amount of moisture in the atmosphere by measuring the amount of water in a theoretical column if all water in that column were to precipitate as rain (kg m^2). This is useful as a variable in the formation of hail, as hail must form through accretion of water onto the surface of a hailstone to grow above the requisite 0.75" to be classified as hail (as defined by the NWS). Therefore, the higher the Precipitable Water, theoretically, the higher chance of hail occurring (although there are instances where this

may not be true). Looking at the size categories, there is a clear trend of decreasing weighted average Precipitable Water as the hail size increases (the outlier being the 2" category). This is interesting, as one would think that more Precipitable Water would mean larger hail sizes. But that does not bear out in the weighted average data, which may be due to the presence of deep tropical moisture in Florida during the summer months, when sea-breeze fronts lead to several small-hail-producing thunderstorms.

As would be expected, the weighted average Precipitable Water decreases at day -1 and day -2, with the values evening out or reversing on day -3 (depending on which hail size category), with an increase in weighted average Precipitable Water. There was more moisture on the day of the hail event, on average, than the day prior to the event (with day -1 having more atmospheric moisture than day -2), with the decreasing atmospheric moisture trend breaking on day -3. This suggests that the weighted average Precipitable Water on day -3 does not have a strong connection to that of day 0 (see Table 2).

The weighted averages for Sea Level Pressure anomaly (SLP) (in Table 3) data show a difference in the variable as hail size varies (moving from <1.00" to 4.00"). The weighted averages of the Sea Level Pressure anomalies consistently fell as hail size increased, up until the 4" category (low sample size of n=1). In other words, the deviation from the climatological norm of Sea Level Pressure grows larger (in the negative) as hail size increases. These data are consistent with what one would expect, as lower Sea Level Pressure theoretically translates to stronger synoptic scale low pressure systems, leading to rising air/instability and the formation

of thunderstorms and hail (also, the lower the pressure, theoretically, translates to more powerful thunderstorms leading to more severe hail.)

Table 2: Precipitable Water (PW, Average) at Various Hail Sizes (Day 0,-1,-2,-3)

Size (inches)	PW, 0	PW, -1	PW, -2	PW, -3
<1	40.06	38.189	37.366	37.4471
1	38.471	36.264	35.6672	35.634
1.25-1.75	37.037	34.845	34.033	32.974
2	37.577	34.204	28.468	33.813
2.25-2.75	33.487	29.445	28.299	28.25
3	29.845	22.68	21.35	26.07
3.25-3.75	28	30	18	12.5
4	25	28	26	24
4.25-4.75	35	30	36.8	22.5

The weighted average Sea Level Pressure anomalies also consistently rose from day 0 to day -3 (again, except for the categories with small sample sizes). These data also line up with what would be expected in theory: the sea-level pressure was, on average, higher on each consecutive day previous to day 0 (day of hail event), all the way up to day -3 (see Table 3)

Weighted averages of Temperature anomalies at 400hPa (T400hPa) (Table 4) follow a recognizable pattern of anomalies becoming more negative as hail size increases (until 2.25-2.75” and after, where sample size is the likeliest explanation of why the pattern breaks). The

400hPa level is located in the upper-middle part of the troposphere, and is also an area where cloud tops reach and where hailstones can begin to form due to water freezing. The lower the temperature at this level, the more likely it would theoretically be for hailstones to form, and moreover, for larger hailstones to initially form, which is consistent with the data in Table 2.

Table 3: Sea Level Pressure (SLP; Anomaly) at Various Hail Sizes (Day 0,-1,-2,-3)

Size (inches)	SLP, 0	SLP, -1	SLP, -2	SLP, -3
<1	-0.672	-0.2447	0.01	0.213
1	-0.914	-0.339	-0.085	-0.085
1.25-1.75	-1.447	-0.779	-0.461	-0.404
2	-1.872	-1.056	-0.754	-0.308
2.25-2.75	-2.427	-1.133	-1.455	-1.055
3	-4.82	-1.325	-0.33	-2.17
3.25-3.75	-8.3	-7.5	-3.3	-4
4	3	1	0	3.5
4.25-4.75	-2	-3	-7	-2

A similar pattern emerges for weighted average temperature anomalies at 400hPa as it has with other variables with regards to the values of the variables in the days prior to a hail event: temperature anomalies became less negative from day 0 to day -2, with the trend largely dissipating or reversing by day -3. This can be interpreted as temperatures, on average, becoming colder at the 400hPa level in the days leading up to a hail event (see Table 4).

Weighted averages of Temperatures anomalies at 500hPa (T500hPa), shown in Table 5, follow a very similar pattern to that of the weighted averages at Temperature at 400hPa. A general, persistent pattern of increasingly negative temperature anomalies is present as hail size increases. This implication, as stated for the Temperature at 400hPa variable, is that temperatures, on average, decrease at the 500hPa level as hail size increases (with the pattern breaking after 3" due to sample size). Compared to the 400hPa temperature levels, the 500hPa temperatures are overall comparable in magnitude with no major *pattern* of variation occurring, although there are sizable differences in some cases as can be seen by referring to Tables 4 and 5. 500hPa is still an area that can be considered the upper-middle level of the atmosphere, where one would expect hailstones to form from the freezing of liquid water. Additionally, temperature anomalies at Temperature at 500hPa on average became less negative in the days prior to a hail event, mimicking the pattern seen for Temperature at 400hPa (see Table 5).

Weighted average Temperatures anomalies become noticeably less negative at the 600hPa level (T600hPa) (Table 6) compared to 500hPa and 400hPa. Although the average temperature anomalies at 600hPa are mostly negative at day 0 throughout all hail sizes, there is no definitive pattern of anomalies becoming more negative as hail size increases, as from <1" to 1.25-1.75", anomalies become more negative, but then reverse and become more positive, with everything over 3" having no pattern at all due to sample size. With overall average temperature anomalies becoming less negative (warmer) at 600hPa, the theoretical amount of available liquid water would increase, which could contribute to hail growth by accretion. This may help to explain why the larger hail sizes with reliable sample sizes show a clear trend of increasingly less negative temperature anomalies starting at 600hPa with increasing hail size, whereas the

smallest hail sizes become more negative with increasing hail size (on average). Smaller size hail would not have the ability to grow through accretion as much as the larger sizes if the temperatures were slightly warmer, on average, for the larger hail at the same level (600hPa). Finally, once again, temperature anomalies at Temperature at 600hPa on average became increasingly negative moving from day 0 to day -3, exactly as the data for Temperature at 400hPa and Temperature at 500hPa showed (see Table 6).

Table 4: Temperature at 400hPa (Anomaly) at Various Hail Sizes (Day 0,-1,-2,-3)

Size (inches)	T400, 0	T400, -1	T400, -2	T400, -3
<1	-0.426	-0.335	-0.272	-0.19
1	-0.459	-0.4	-0.277	-0.251
1.25-1.75	-0.725	-0.491	-0.313	-0.253
2	-0.935	-0.48	-0.36	-0.416
2.25-2.75	-0.662	-0.418	-0.466	-0.029
3	-1	-0.578	-0.49	0.175
3.25-3.75	-1	-0.5	0	0.5
4	-6	-4	-3.5	-2
4.25-4.75	2	2.5	3	0

Table 5: Temperature at 500hPa (Anomaly) at Various Hail Sizes (Day 0,-1,-2,-3)

Size (inches)	T500, 0	T500, -1	T500, -2	T500, -3
<1	-0.412	-0.231	-0.098	-0.069
1	-0.494	-0.357	-0.218	-0.078
1.25-1.75	-0.83	-0.484	-0.314	-0.19
2	-0.763	-0.484	-0.168	-0.32
2.25-2.75	-0.844	-0.377	-0.102	-0.16
3	-1.088	-0.165	-0.16	-0.16
3.25-3.75	-0.5	-1	-0.5	-0.5
4	-6.5	-3.5	-2	-2
4.25-4.75	1.5	2.5	2.5	0

In Table 7, the weighted average of temperature anomalies at 850hPa (T850hPa), the data are significantly different compared to temperatures at other pressure levels. Overall, temperature anomalies were increasingly positive as hail size increased on day 0. As stated in the previous paragraph, the overall warmer temperature at middle and lower levels of the atmosphere may lead to hail growth through accretion more easily through more available liquid water (as opposed to frozen water), leading to larger hail sizes. The temperature variations between the upper, middle and lower levels of the atmosphere are crucial to the growth of hail, as updrafts will carry hailstones up through these layers, where they will freeze, fall, grow through accretion, and repeat, forming larger hailstones (Longley and Thompson 1965). At larger hail sizes (>2”), temperature anomalies, on average, were greater than 1°C (with the exception of the 4” category, with sample size n=1) (see Table 7).

Table 6: Temperature at 600hPa (Anomaly) at Various Hail Sizes (Day 0,-1,-2,-3)

Size (inches)	T600, 0	T600, -1	T600, -2	T600, -3
<1	-0.352	-0.07	-0.012	-0.01
1	-0.417	-0.239	-0.165	-0.085
1.25-1.75	-0.608	-0.342	-0.209	-0.086
2	-0.556	-0.161	-0.123	-0.218
2.25-2.75	-0.379	0.055	-0.19	-0.171
3	0.495	1.165	-0.16	0.005
3.25-3.75	-0.5	-1	-1.5	1
4	-6	-4	-2.5	-2.5
4.25-4.75	3	3	2.5	0

Lastly, temperature anomalies, on average, become less positive from day 0 to day -3. This contrasts with the other three layers (Temperature at 400hPa, Temperature at 500hPa, Temperature at 600hPa), where temperatures became less negative form day 0 to day -3. While this can be considered a "contrast", temperature anomalies, on average, became less *extreme* from day 0 to day -3 (temperature anomalies converge to 0, meaning only slight deviation from the mean climatological temperature) (see Table 7).

As seen in Table 8, a clear pattern can be seen as vector wind averages at 200hPa (VW200hPa) increase dramatically as hail size increases (with the lone exception of the 4" hail). Vector Wind at 200hPa does not, however, only increase for day 0 as hail size increases, but the pattern also holds for day -1, day -2 and day -3. The increase in wind as hail size

increases at 200hPa (upper level) could suggest that a stronger jet is present on the synoptic scale at larger hail sizes, which would be conducive to the formation of stronger thunderstorms.

Table 7: Temperature at 850hPa (Anomaly) at Various Hail Sizes (Day 0,-1,-2,-3)

Size (inches)	T850, 0	T850, -1	T850, -2	T850, -3
<1	0.746	0.682	0.209	0.174
1	0.905	0.609	0.403	0.314
1.25-1.75	0.853	0.743	0.428	0.279
2	1.011	0.73	0.222	-0.022
2.25-2.75	1.379	1.084	0.709	-0.105
3	0.825	0.99	0.66	0.34
3.25-3.75	3	3.5	3.5	-2
4	-2	0	-0.5	-2
4.25-4.75	5.5	5	4	1.5

Interestingly, from day 0 to day -3, there is little change in the average Vector Wind at 200hPa. This can at least be partially explained by looking at the data used to create Table 8. The Vector Wind is highly dependent on season, which is not taken into account in this analysis. During the summer months, the Subtropical Jetsteam shifts north, weakening the strength of upper level winds near Florida (temperature and pressure gradient is decreased drastically in summer as both the high latitudes and low latitude receive enough solar radiation). As seen from Figures 3-6, the largest hail sizes occur primarily in the late winter and spring

(February-May) (when the Subtropical Jet is closer or may even be over Florida), while smaller hail sizes are numerous in the summer months (June, July and August).

Table 8: Vector Wind (Average) at 200hPa at Various Hail Sizes (Day 0,-1,-2,-3)

Size (inches)	VW200, 0	VW200, -1	VW200, -2	VW200, -3
<1	12.765	12.238	11.918	12.373
1	13.572	13.494	13.508	13.8
1.25-1.75	19.174	18.745	18.846	19.124
2	17.532	18.787	19.657	19.778
2.25-2.75	33.349	33.721	32.728	33.719
3	43.33	39.03	43.67	37.98
3.25-3.75	52.5	50	55	52.5
4	34	33	27	24
4.25-4.75	62.5	57.5	62.5	50

In Table 9, the Vector Wind average at 300hPa (VW300hPa), the weighted average of the hail files yields unsurprising results. The trend of increasing Vector Wind magnitude as hail size increases mimics the trend seen in Table 8 for Vector Wind at 200hPa. The one major, obvious, difference is that the magnitude of the Vector Wind at 300hPa, for every hail size, is smaller than that of Vector Wind at 200hPa. This is easily explained by the phenomenon of friction, as there is less air present at 200hPa as there is at 300hPa. Therefore, because there is more air friction at 300hPa, the wind speeds should, theoretically, not be as large as those at 200hPa (which the data clearly agrees with). Additionally, just as at Vector Wind at 200hPa,

Vector Wind at 300hPa the Vector Wind did increase in magnitude with hail size not just on day 0, but day -1, day -2 and day -3. The Vector Wind at 300hPa also did not vary greatly moving from day 0 to day -3 for all hail categories (except the largest), following the trend seen at Vector Wind at 200hPa (although the day 0 value is higher, in most cases, than the Vector Wind at day -1, day -2 and day -3).

Table 9: Vector Wind (Average) at 300hPa at Various Hail Sizes (Day 0,-1,-2,-3)

Size (inches)	VW300, 0	VW300, -1	VW300, -2	VW300, -3
<1	9.173	8.8	8.866	9.008
1	10.946	10.793	10.948	11.188
1.25-1.75	14.523	14.141	14.112	14.084
2	13.589	13.678	14.861	14.745
2.25-2.75	25.796	26.421	25.592	24.713
3	34.33	30.05	33.35	31.805
3.25-3.75	40	35	41	41
4	26	20	14	17
4.25-4.75	47.5	47.5	42.5	42.5

The Vector Wind average at 500hPa (VW500hPa) (Table 10) sees little change from the pattern seen for Vector Wind at 200hPa and Vector Wind at 300hPa. The magnitude of the Vector Wind at 500hPa, compared to that of Vector Wind at 200hPa and Vector Wind at 300hPa, is lower, which is, again, explained by air friction. A clear pattern is emerging from

observing the Vector Wind at 200hPa, 300hPa and 500hPa: Vector Wind increases in magnitude as hail size increases (not only on day 0, but day -1, day -2 and day -3). In addition, Vector Wind still does not vary greatly moving from day 0 to day -3, although the Vector Wind on day 0 is slightly larger.

Table 10: Vector Wind (Average) at 500hPa at Various Hail Sizes (Day 0,-1,-2,-3)

Size (inches)	VW500, 0	VW500, -1	VW500, -2	VW500, -3
<1	6.073	5.381	5.453	5.339
1	6.682	6.593	6.898	6.97
1.25-1.75	9.35	8.432	8.308	8.231
2	9.101	8.317	8.556	8.58
2.25-2.75	15.303	14.188	14.654	14.597
3	20.3	14.67	16.01	18.94
3.25-3.75	22.5	22.5	23.5	25.5
4	15	11	11	10
4.25-4.75	26.3	32.5	28.8	21.3

Vector wind averages at 700hPa (VW700hPa) (Table 11) follow a similar pattern seen from the 200-500hPa levels. Again, the magnitude of the Vector Wind increased as hail size increased (with the one exception once again being the 4”) for day 0, day -1, day -2 and day -3. Other patterns discussed between Vector Wind at 200hPa, 300hPa and 500hPa were also present in the data for Vector Wind at 700hPa, with the notable exception being a more noticeable drop-off in Vector Wind magnitude from day 0 to day -1. Previously, the drop-off in

magnitude between day 0 and day -1 for Vector Wind at 200hPa-500hPa was small or non-existent; but here, we see a clear and consistent drop-off in magnitude for all hail inch size categories, with day -2 and day -3 following no clear pattern. The change in this particular pattern may be explained by the forces that dictate weather in this area of the atmosphere. In the upper levels (200-500hPa), winds are dictated by large synoptic or global scale phenomenon, such as the jet stream and general increase and decrease of temperature/pressure gradients with respect to season. Now, at 700hPa, the mid-levels of the atmosphere, winds patterns are more influenced by weather features such as cold fronts, warm-core cyclones (tropical systems), most thunderstorms and other smaller scale synoptic or mesoscale weather phenomena.

Table 11: Vector Wind (Average) at 700hPa at Various Hail Sizes (Day 0,-1,-2,-3)

Size (inches)	VW700, 0	VW700, -1	VW700, -2	VW700, -3
<1	3.81	3.17	2.952	2.92
1	4.372	3.129	3.87	3.905
1.25-1.75	5.58	4.789	4.701	4.51
2	5.363	4.305	4.433	4.78
2.25-2.75	9.447	8.407	8.509	7.813
3	11.785	4.01	7.165	10.28
3.25-3.75	14.3	14	14	18.5
4	7	6	7	4
4.25-4.75	15.5	18	18	11

At 850hPa (VW850hPa) (Table 12), the pattern for Vector Wind average follows the same pattern as that of the Vector Wind at 700hPa, except that the decrease in magnitude from day 0 to day -1 from the 700hPa can now be extended out to day -2 and day -3 in the majority of hail size categories at the 850hPa level. This shift can be attributed, as previously stated, by the influence of weather phenomena at this level that have a smaller effect on weather in the upper levels of the atmosphere (fronts, tropical systems, etc.). Thunderstorms are much more likely to be present in the middle and lower levels of the atmosphere, with only the strongest storms reaching above the 500hPa pressure surface. Therefore, it is consistent with what would be expected that the Vector Wind is stronger on day 0 than on day -1, etc. Other than this, Vector Wind at 850hPa follows the same pattern and reasoning at that Vector Wind at 700hPa does.

Table 12: Vector Wind at 850hPa (Average) at Various Hail Sizes (Day 0,-1,-2,-3)

Size (inches)	VW850, 0	VW850, -1	VW850, -2	VW850, -3
<1	2.939	2.447	2.386	2.073
1	3.393	2.759	2.638	2.722
1.25-1.75	4.028	3.332	3.14	2.946
2	3.8	2.509	2.555	2.877
2.25-2.75	6.136	5.243	5.619	5.084
3	8.97	2.98	3.33	6.65
3.25-3.75	8	11.5	7	11.5
4	3	3	4	3
4.25-4.75	10	10.5	10.5	4

In Table 13, we see the Vector Wind at 925hPa averages (VW925hPa). With respect to hail size, the Vector Wind at 925hPa follows the same pattern set previously by Vector Wind at 850hPa (increasing in magnitude as hail size increases). However, when comparing Vector Wind at 850hPa and Vector Wind at 925hPa, the magnitude of the Vector Wind from <1 to 1.25-1.75" did not decrease, but actually slightly increased. At the 925hPa, during a hail event, winds inside of the thunderstorm or just above the surface will be comparable to those at the 850hPa pressure surface, so the trend of winds decreasing with height would be expected to taper off as seen in the data. Other than this change, the patterns seen at Vector Wind at 850hPa in Table 12 are observed at Vector Wind at 925hPa.

Table 13: Vector Wind at 925hPa (Average) at Various Hail Sizes (Day 0,-1,-2,-3)

Size (inches)	VW925, 0	VW925, -1	VW925, -2	VW925, -3
<1	3.055	2.81	2.324	2.177
1	3.502	2.691	2.453	2.797
1.25-1.75	3.625	3.13	2.89	2.495
2	3.332	2.155	2.04	2.234
2.25-2.75	5.105	3.735	4.746	4.627
3	7.655	4.31	2.335	5.65
3.25-3.75	8.5	9.5	6	7.5
4	2	2	5	6
4.25-4.75	8.5	5.5	6.5	2

Finally, at the surface (VWSFC) (Table 14), Vector Wind averages marginally increase with hail size, but increase more so for the larger hail sizes than the smaller ones at day 0 (the one exception being 1.25-1.75"). Also, the Vector Wind magnitudes are considerably smaller than those seen at Vector Wind at 850hPa and Vector Wind at 925hPa (where the magnitude of the Vector Wind did not change much between the two). This can be attributed mostly to surface friction (trees, manmade structures, etc.) However, the trend of Vector Wind magnitude decreasing from day 0 to day -3 remains the same, as the average Vector Wind magnitude on the day of the event is overall larger than that of days prior, most likely due to the presence of hail-producing thunderstorms that produce strong winds.

Table 14: Vector Wind at the Surface (Average) at Various Hail Sizes (Day 0,-1,-2,-3)

Size (inches)	VWSFC, 0	VWSFC, -1	VWSFC, -2	VWSFC, -3
<1	1.584	1.354	1.228	1.192
1	1.766	1.32	1.344	1.341
1.25-1.75	1.715	1.562	1.318	1.201
2	1.994	1.362	1.539	1.683
2.25-2.75	2.581	1.78	2.421	2.287
3	5.165	2.66	2.005	4.33
3.25-3.75	4	4.5	4	5.5
4	2	2	4	6
4.25-4.75	4	2	2	2

Statistical Analysis on Correlation of Variables Using SPSS: Month Groupings

The following tables in Section 3.4 and 3.5 were created using SPSS 21. These tables display correlations between the variables using a bivariate correlation (Pearson, two-tailed). The first three sets of tables provides an analysis of the NCEP/NCAR Reanalysis data used to analyze the correlations between the different variables for each month grouping. This was done to analyze any differences in the correlations between variables based on seasons in Florida. For this exercise, the data from every file for February-May (every region and hail size), then June-September and finally October-January was uploaded into SPSS 21 and used to perform the bivariate correlation. These analyses were done only for day 0, the day of the hail event.

Each "row" consists of a variable and has three portions, while each vertical column also consists of one of the variables used. For the three portions of the rows, the Pearson Correlation number appears at the top, which ranges from -1 to 1. A value of -1 represents a perfectly negative correlation with the other variable, while a value of 1 represents a perfectly positive correlation. A value of 0 represents no correlation. The second portion of the row is the sigma value, which determines the statistical significance of the Pearson Correlation number. If sigma is less than .05, there is 95% confidence in the Pearson Correlation value given (denoted by an asterisk *). If sigma is less than .01, there is a 99% confidence in the Pearson Correlation number given (denoted by a double asterisk **). Finally, N is the sample size (number of files used – each file containing the average of several hail events).

Month Grouping: February-May

In Tables 15 and 16 (see Appendices), starting with the Lifted Index, there are some notable correlations with other variables in the February-May month grouping. Lifted Index has a fairly strong positive correlation with T400hPa, T500hPa and T600hPa. It is no surprise that Lifted Index correlates with these variables, as they are used in the calculations to determine the Lifted Index. In summary, as average Lifted Index increases (or decreases), so do temperature anomalies at 400hPa, 500hPa and 600hPa. A lower value of Lifted Index would suggest more instability and the potential for stronger thunderstorms (and therefore hail), while lower temperatures at 400, 500 and 600hPa would be ideal for the initial formation of hailstones. Lower temperatures in the atmosphere may also indicate the presence of a cooler air mass (front) moving through, giving way to the violent thunderstorms Florida encounters due to frontal systems during these months.

Lifted Index also has a somewhat weak, positive correlations with the Vector Wind at both upper-levels and lower-levels of the atmosphere, but not mid-levels for this month grouping. This may be explained by the tendency of Lifted Index to be more negative in the summer months than in the winter months. In the month of February, for example, the average Lifted Index is much higher than in May. But, in May, frontal systems are not as common as the late winter and early spring in Florida. Therefore, there may be a higher Lifted Index in a month such as March as well as stronger upper-level and lower-level winds from the passage of a frontal system, while the Lifted Index could be lower in May with hail forming from sea-breeze fronts with lighter winds at the upper and mid-levels. This is only one, possible way to justify

the existence of the weak to moderate positive correlation between Lifted Index and the various Vector Wind variables.

The only meaningful, strong correlation average Precipitable Water has with any variable in this month grouping is a positive correlation with temperature anomalies at the 400, 500 and 600hPa levels (the strongest being 400, then 500, then 600 respectively). From a meteorological standpoint, this makes sense, as a warmer temperature would allow for more Precipitable Water in the column compared to colder temperatures, as warmer air can hold more water than colder air.

Sea Level Pressure anomalies are observed to have a negative correlation with temperature anomalies at all levels measures (400hPa, 500hPa, 600hPa and 850hPa). This suggests that when Sea Level Pressure is lower than normal, temperatures at the various levels of the atmosphere are warmer than normal. This makes sense synoptically, as, during the spring months, warmer air is drawn from south to north ahead of cold fronts and low pressure systems that accompany them, translating to warmer air and falling pressure on hail days. The other Sea Level Pressure correlation is also a negative correlation with Vector Wind at the middle and lower levels of the atmosphere. A negative (positive) Sea Level Pressure anomaly could indicate the presence of a nearby low (high) pressure, which could be responsible for a pressure gradient and therefore stronger (lighter) winds. Additionally, as the Sea Level Pressure decreases, the Vector Wind at the surface will increase, and vice versa. Less surface pressure would also mean there is less air at the surface, translating to less air friction and stronger winds, although this would have only minimal impact at the surface.

Overall, the four temperature variables (Temperature from 400-850hPa) have a possible correlation with Lifted Index and Precipitable Water, but negative correlation to Sea Level Pressure as discussed previously. Obviously, the temperature variables would all have correlations among themselves as well, which is shown in the data. Additionally, the temperature variables appear to be correlated positively with Vector Wind overall. Specifically, moving from the upper atmosphere towards the surface, temperature becomes more positively correlated with magnitude of the vector wind (with the exception of Vector Wind at Surface). Furthermore, the positive correlations between temperature and vector wind appear to increase moving from Temperature 400-850hPa (a few of these correlations are not statistically significant, but overall, this is the trend in the data.) This would suggest that warmer temperatures lead to higher wind magnitudes, specifically closer to the surface.

A number of factors could explain the positive correlation between temperature and vector wind magnitudes. Above the surface, wind speeds are generally higher due to less friction (less air). Given an arbitrary volume of warmer air against that same volume of colder air (all other things being constant), the warmer air would be less dense and therefore lower pressure, causing wind to encounter less friction and theoretically faster. Additionally, warmer air is less stable than cooler air, which may lead to the warmer air rising and potentially developing localized storms with accompanying stronger winds (Farley et al. 2004).

Finally, and obviously, the numerous Vector Wind variables all have positive correlations to one another, as they all measure the same thing, just at various levels of the

atmosphere. If winds are relatively strong at 200hPa, it is likely that subsequent areas of the atmosphere would also have stronger winds.

Month Grouping: June-September

The wet season (summer months) brings with it drastic changes in synoptic patterns that greatly affect atmospheric variables, as seen in Tables 17 and 18 (see Appendices). In the late winter and spring months, Lifted Index had many positive correlations with temperature variables and Vector Wind variables. However, in the summer, Lifted Index was found to have only one strong, negative, correlation with Temperature at 850hPa, meaning that Lifted Index decreases when temperature anomalies at 850hPa are positive. Fronts rarely pass through Florida during the summer (those that pass are usually very weak), so thunderstorms are typically caused by the sea breeze(s), the strong negative correlation can be explained by latent heat release. At 850hPa, warm air rising adiabatically would cause the water vapor in the air to begin to condense and release heat. It is this condensation which would lead to rain and thunderstorms. Recalling that a lower Lifted Index would translate to less stability (and a stronger likelihood of storms), it would make sense that a lower Lifted Index would be strongly correlated with an increase at temperatures at 850hPa, and vice versa.

Precipitable Water has no statistically significant correlations with temperature anomalies in the summer, unlike in the late winter and spring. However, the data shows that it does have a strong negative correlation with Vector Wind at 200hPa and Vector Wind at 300hPa (upper level winds). This would indicate less average Precipitable Water when the

Vector Wind is stronger at the upper levels. Recall that winds during the summer are usually uniform throughout the atmosphere (low wind shear) due to the jet stream moving northward. However, this does not mean the jet stream never moves southward toward Florida, especially in September. The jet stream would not only bring higher upper level winds with it, but possibly a drier air mass, leading to less Precipitable Water, which may explain this negative correlation.

Sea Level Pressure did not show much in the way of correlations with any other variables during the summer months. Most correlations are small, and nearly all are statistically insignificant. This would be expected in the summer months, as pressure is uniformly low in Florida during the summer with little baroclinic variability.

Additionally, the temperature variables had only few statistically significant correlations with other variables (besides other temperature variables). The few that did showed a statistically significant correlation near 0, which indicates little to no correlation (with the glaring exception of Lifted Index and Temperature at 850hPa discussed above). Of course, many of the Vector Wind variables also have strong positive correlations among themselves.

Month Grouping: October-January

The fall and early winter brings further change to the relationship between variables on hail days in Florida. Lifted Index has a drastically different relationship, as seen on the data in Tables 19 and 20 (see Appendices). Lifted Index has a very strong negative correlation with Sea Level Pressure anomalies in these months, meaning that lower Lifted Index tends to have higher

pressure. This seems to be an unusual observation. However, it may be related to the strongly positive correlation that average Lifted Index has with all of the Vector Wind variables. As Lifted Index increases during this month grouping, Vector Wind magnitude also tends to increase and vice versa. This could be due to the drastic seasonal changes seen within this month grouping. In the early part of the month grouping (October and November), the jet stream usually is not over Florida as much as during the heart of the winter months (December and January). This would lead to less overall wind speeds, especially at upper levels (200hPa and 300hPa) in October and November (similar to the summer months which have little wind shear) and stronger wind speeds in the winter months (December and January) due to the jet stream pushing south near and over Florida. Also, during the summer months, the Lifted Index tends to remain steadily low over Florida with the persistence of warm, tropical air masses and little day-to-day pressure and temperature changes. Compare this to the winter months, where cooler, more stable air masses move in from the north (leading to higher Lifted Index). Therefore, the stronger winds and higher Lifted Index during the winter months (December and January) compared to the lower wind speeds and lower Lifted Index of the months directly proceeding the rainy season (October and November) could explain the strong positive relationship between Lifted Index and the Vector Wind variables during this month grouping. Precipitable Water has no statistically significant correlations with any of the other variables, or has statistically significant correlations with values near 0.

Sea Level Pressure, according to the data, has a statistically significant negative correlation with Temperature at 500hPa, but does not with any of the other temperature variables. This seems plausible, as lower mid-level temperatures, especially in the winter, often

correspond with high pressure. However, it is noted that no other temperature variables show statistically significant results. The other major variables that Sea Level Pressure shows a correlation with are the Vector Wind variables. Sea Level Pressure shows significant and strong negative correlations with all Vector Wind variables, which indicates lower than average Sea Level Pressure when there are stronger winds and vice versa. This can be explained by the fact that, during these months, frontal and low pressure systems move through Florida. These systems tend to bring strong winds and thunderstorms (which can contain hail) ahead of the front. Just ahead of the cold front, there will typically be both lower pressure and strong, southerly winds accompanied by thunderstorms, providing the negative correlation between Sea Level Pressure and the Vector Wind seen in the data below. The temperature and vector wind variables had little in the way of statistically significant correlations that were positive or negative that were not covered above.

Statistical Analysis on Correlation of Variables Using SPSS: Regions

Northwest Florida Region

Tables 21 and 22 (see Appendices) show the correlations between atmospheric variables during Florida hail days in the Northwest region of Florida. Looking at Lifted Index, there is a negative correlation with Precipitable Water. This makes sense, as the Lifted Index should decrease (a less stable environment) when there is more average Precipitable Water (which would also mean higher humidity). The more water in the air, typically, the more unstable the environment is. However, once again, the strong negative correlation between Sea Level

Pressure and Lifted Index is unusual, as stated in the section regarding the October-January month groupings (Tables 19 and 20). But, once again, it may be affected by the strong positive correlation between Lifted Index and the magnitude of the Vector Wind variables (also described above and observed in Tables 19 and 20).

Precipitable Water, besides Lifted Index, has many other correlations. The positive correlation between Precipitable Water and Sea Level Pressure theoretically makes sense, as less pressure means there is less mass in a column of air extending from the surface to the top of the atmosphere, which would also mean there were less water molecules to create Precipitable Water with. Precipitable Water also had a very strong negative correlation with the Vector Wind variables. As stated in the last section, there are generally stronger winds, especially at the upper levels, in the winter compared to the summer in Florida due to the movement of the jet stream. The jet stream brings stronger winds at all levels of the atmosphere, as well as frontal systems and often drier air masses behind it, which would lead to less Precipitable Water.

Sea Level Pressure similarly has a negative correlation with the Vector Wind variables, meaning that higher pressure translates to lower wind speed and vice versa. This would make sense, as generally, lower pressure is accompanied by more instability, the chance for thunderstorms, and less air friction, which all lead to higher wind speeds.

The temperature and vector wind variables have no additional correlations, except of course for the correlations among the temperature variables with themselves and the Vector Wind variables with themselves.

Northeast Florida Region

Table 23 and 24 (see Appendices) comprise the data on the correlations between the different atmospheric variables on hail days in the Northeast region of Florida. Compared to the Northwest region of Florida, the Lifted Index correlates to other variables in the Northeast region. Lifted Index correlates negatively to Precipitable Water and Sea Level Pressure, with the reasoning behind the correlations the same as their Northwest counterparts (or lack thereof in the case of Lifted Index and Sea Level Pressure correlation). There is also a positive correlation between Lifted Index and the Vector Wind variables for the same reason described above for the Northwest Region seen in Tables 21 and 22. The one area of notable difference between these two regions, however, is that Lifted Index has statistically significant positive correlations with both Temperature at 500hPa and 850hPa, as well as positive correlations with Temperature at 400hPa and 600hPa that are just under the criteria to qualify for statistically significant. Simply, positive temperature anomalies translate to higher Lifted Index (more stability) according to the data.

With regards to Precipitable Water, Northeast Florida has the same negative and positive correlations to Lifted Index and Sea Level Pressure, respectively, which Northwest Florida does for the same reasons. It is worth noting that the Northeast correlations are significantly stronger than those in Northwest Florida. Precipitable Water in the Northeast also has the same negative correlations to the Vector Wind variables in the Northwest, albeit not as strong. The difference once again comes to temperature, where there is a significant negative correlation between Precipitable Water and Temperature at 850hPa. Geography may play a role in this difference.

The Northeast region of Florida contains far more interior counties than coastal areas, and receives less hail-producing thunderstorm activity due to sea-breeze fronts than areas on the Florida Peninsula or closer to the coast. Therefore, these areas would receive more hail from cold frontal systems, which could explain the negative correlation between Temperature at 850hPa and Precipitable Water (more Precipitable Water while Temperatures at 850hPa are cooler than normal due to the cold front).

Other than Lifted Index and Precipitable Water, Sea Level Pressure has statistically significant negative correlations with Vector Wind in the Northeast region just as the Northwest region does. However, the main difference between the two regions is Temperature at 850hPa. It would make sense, theoretically, that lower Sea Level Pressure would translate to higher Temperatures at 850hPa, especially in the summer when Sea Level Pressure is normally low and latent heat release from condensation of summer storms during the day would lead to higher Temperature at 850hPa. There are no other statistically significant correlations with other temperatures, perhaps due to summer storms not often reaching heights over 700hPa and therefore not releasing latent heat due to condensation as it does at 850hPa.

It appears that the temperature variables have some positive correlation to the Vector Wind variables in the Northeast region, especially Temperature at 850hPa. Temperature at 400hPa, 500hPa and 600hPa all have sporadic, statistically significant, positive correlations with the Vector Wind variables, though it is not consistent through the upper, mid or low levels such as Temperature at 850hPa. This may have to do with the stronger contrasting temperatures in Northeast Florida than Northwest Florida. Northwest Florida is comprised of mostly coastal

counties, whereas Northeast Florida has several interior counties. The inland counties are much hotter in the summer than coastal counties, and much colder in the winter than coastal counties (due to high specific heat of water in the ocean keeping coastal counties more mild) contributing to stronger sea breeze effects (higher winds and latent heat release from sea breeze storms at 850hPa).

Central Florida Region

Tables 25 and 26 (see Appendices) show the data for the correlations between atmospheric variables in Central Florida during hail days. The Lifted Index correlations mirror that of the Northeast, with the exception of the temperature variables. Like the Northeast Region, Central Florida does have a positive correlation to Temperature at 850hPa, but lacks the statistically significant correlations to Temperature at 400hPa, 500hPa and 600hPa.

Precipitable Water in Central Florida, however only mirrors the Precipitable Water in Northeast Florida with regards to Lifted Index (as discussed above) and the Vector Wind variables. Precipitable Water does not share a statistically significant correlation with Sea Level Pressure as it does in Northeast and Northwest Florida, unless one were to use a 90% confidence interval. This weak and statistically insignificant correlation (by the criteria of this study) may be weaker than that of the Northwest and Northeast due to the tendency of lower pressures during the summer, when sea-breeze fronts bring multiple hail-producing thunderstorms. Although the same phenomenon is seen in both Northeast and Northwest Florida, it is not as prominent nor as powerful as it is in Central Florida due to the region

experiencing daily clashes between the sea breeze from the Gulf of Mexico and the Atlantic Ocean. Precipitable Water also has a negative correlation with Temperature at 850hPa, although is barely meets the criteria for a 5% level.

Sea Level Pressure anomaly correlations in Central Florida also mirror the Sea Level Pressure anomaly correlations in Northeast Florida, except for with Precipitable Water (discussed above). Out of all of the temperature anomaly correlations in Central Florida, only Temperature at 850hPa stands out as having strong, positive correlations with all of the Vector Wind variables, while the other temperature variables have either no statistically significant correlations or very weak (near 0) significant correlations, similar to Northeast Florida.

South Florida Region

Finally, Tables 27 and 28 (see Appendices) reflect correlations between atmospheric variables in South Florida on hail days. Average Lifted Index sees the same correlations observed in Central Florida and Northeast Florida throughout for the same reasoning as stated in the other sections, with the exception of Temperature at 850hPa, where there is no correlation in South Florida. This may be due to South Florida's tropical climate. South Florida, due to its geographic location, tends to have lower Lifted Index throughout the year than the other regions as cooler, more stable air (and the higher Lifted Index that accompanies it) from fronts rarely reaches the area. With the overall uniformity in atmospheric temperatures, pressures and wind throughout the year in this tropical climate, it is feasible that Lifted Index would not have correlations with temperature at various heights.

Precipitable Water correlations in South Florida also show the same correlations as they do in Central Florida with respect to Vector Wind and Lifted Index (discussed previously) for the same reasons stated in the Central Florida section. However, Precipitable Water in South Florida exhibits a positive correlation with Temperature at 400hPa, 500hPa and 600hPa, excluding 850hPa. The previous regions showed correlations with Temperature at 850hPa, and not the other temperature variables, a complete reverse as seen in the tables below. This suggests that higher temperatures at upper to middle levels of the atmosphere relate to increased Precipitable Water in South Florida. This can be explained by the movement of the tropopause (the delineation between the troposphere and stratosphere) through the seasons, where the tropopause rises during the summer and sinks during the winter. Generally, warmer air underneath the tropopause will cause it to rise, and cooler air will cause it to sink. Warmer temperatures at Temperature at 400-600hPa would indicate a higher tropopause (summer), when Precipitable Water would be higher than it would be during the winter due to prevailing warm, tropical air masses in the summertime.

Statistically significant Sea Level Pressure anomaly correlations with other variables on hail days in South Florida also show a distinction with the other regions, as Sea Level Pressure is negatively correlated with Temperature at 400hPa, 500hPa and 600hPa (and almost 850hPa, where the confidence level is at 94.9%, just under the 95% requirement for confidence). This phenomenon may also be explained by the movement of the tropopause as described previously. Sea Level Pressure is often lower during the summer months when the tropopause is higher (meaning warmer temperatures throughout the atmosphere), leading to the positive correlation.

Unlike the other regions, Sea Level Pressure does not have a statistically significant correlation with the Vector Wind variables in South Florida. Due to little Sea Level Pressure and Vector Wind magnitude variance during the summer (when most hail days occur in South Florida), it is unsurprising that there is no correlation. The temperature variables, of course, have correlations between each other, but have no significant correlations with the Vector Wind variables on hail days in South Florida.

Objective 1 Discussion

"*To create a full understanding of the atmospheric variables which impact hail formation and hail events in Florida through use of the NOAA archives and NCEP/NCAR Reanalysis data of days of hail events and days leading up to hail events."*

It is difficult to create a "full" understanding of all of the possible variables which impact hail formation and events in Florida, however, analyzing the variables throughout Section 3 may improve understanding of the variables and their effects. The use of NOAA archives and NCEP/NCEP Reanalysis maps played a crucial role in determining how the variables and their relationships affect the formation of hail.

Throughout all of the composite NCEP/NCAR Reanalysis maps, it is clear a low Lifted Index, in most cases, is present during most hail days in Florida. Days which had high Lifted Index values on the days of hail events were during the fall and winter months, when Lifted Index is higher due to cooler, more stable airmasses prevailing over Florida, compared to the

warmer tropical airmasses of summer (less stable). In the days leading up to a hail event, Lifted Index was almost universally higher than the day of the event. This comes as no surprise, as Lifted Index is a measure of instability, and an unstable environment breeds the thunderstorms necessary for hail development.

The composite NCEP/NCAR maps also showed that, on hail days, Precipitable Water is often higher than it was in the previous days, sometimes quite significantly. This is again not a surprise, as more Precipitable Water could suggest more moisture available for thunderstorms to form and increase the likelihood of storms containing hail (depending on where in the atmosphere the moisture is concentrated). Too much moisture throughout the entire atmospheric column would not be conducive to hail formation.

The only other major, universal theme throughout the NCEP/NCAR Reanalysis maps is that negative Temperature anomalies at 400hPa, 500hPa and 600hPa almost always corresponded to positive Temperature anomalies at 850hPa anomalies on the day of a hail event, while the days leading up to a hail event would have much weaker temperature anomalies at the various pressure levels. There are several reasons for this commonality between all regions and month groupings. A positive temperature anomaly observed at 850hPa during a hail event can be justified by latent heat release through condensation of water droplets due to condensation at this level, while there would be much less at higher pressure levels. The more condensation, the more latent heat is released and the stronger the likelihood of rain and hail events. Additionally, the warm temperature anomalies may suggest an area where the moisture in the atmosphere, seen in the high Precipitable Water values, may be located. It is no

coincidence that larger hail size was also associated with the highest temperature anomalies at 850hPa. Additionally, cooler temperature above the 850 levels, closer to the top of clouds, may help provide sufficiently cold temperatures for initial formation of hailstones. These hailstones would then fall and grow through accretion, probably around the 850hPa level where there are warmer temperatures and liquid water. Subsequent updrafts would push the hailstone up again to refreeze in the cooler heights of 400hPa, 500hPa or 600hPa. If temperatures at the higher altitudes (400hPa, 500hPa and 600hPa) were found to have warmed along with the 850hPa level, this would indicate a deeper tropical air mass (which is not the case in the data).

Objective 2 Discussion

"To use the knowledge of atmospheric variables for each specific region, month grouping and hail size distribution to determine which factors are most critical for the formation of hail in different regions of Florida through various seasons."

The values of atmospheric variables, as well as their relationships, vary greatly between hail size, month groupings and seasons. These were all discussed throughout Section 3.0. While all of the variables play some role in the occurrence of a hail day, it is important to observe the various correlations seen in Sections 3.4 and 3.5.

With respect to hail size, the data show that Lifted Index increases with larger hail sizes, while Precipitable Water decreases with larger hail sizes. At first glance, this would not seem to make sense as more instability and more Precipitable Water could lead to larger hail, especially

when referring to other regions such as the Midwest United States. However, in Florida, the majority of hail falls during the summer months and is caused by sea breeze fronts, not frontal systems passing through. Additionally, summer hail is usually small, while large hail is more often associated with fall and spring frontal systems with stronger updrafts to create larger hailstones. Lifted Index is always much lower in the summer in Florida, and Precipitable Water is generally higher as seen in the NCEP/NCAR Reanalysis images. Therefore, while in most other regions of the country one would usually expect lower Lifted Index with higher hail inch sizes and possibly higher Precipitable Water with higher hail inch sizes, Florida's unique subtropical and tropical climates with higher temperatures and more tropical airmasses lead to the opposite observation, especially in the summer months. Other findings include increased Vector Wind magnitude with increased hail size, which would be expected as stronger updrafts help to lift hail higher into the atmosphere, where it can freeze and fall through areas of high humidity and super-cooled water to accrete more water onto the surface, creating a larger hailstone.

With respect to the month groupings, it is clear that factors leading to hail development are very different from season to season in Florida. The most notable differences are seen when comparing the rainy season (June-September) with the other two month groupings. One of the most important findings during this period is that Temperature at 850hPa anomalies tend to be positive during hail days. While it is generally true that Temperatures at 850hPa may be positive during hail days, it is especially pronounced during the summer month grouping due to deep, moist, rising, tropical air condensing at around 850hPa and releasing latent heat, and producing the observed anomaly (a strong negative correlation between Lifted Index and Temperature at 850hPa was observed). This anomaly is much less pronounced in the February-May month

grouping (with October-January being a strange case). Additionally, other temperature anomalies at different heights (Temperature at 400hPa, 500hPa and 600hPa) were correlated to Lifted Index, Precipitable Water, and Sea Level Pressure (colder temperatures at those heights may be more conducive to hail formation by creating the necessary freezing layer, and were correlated to lower average Lifted Index, higher average Precipitable Water and lower Sea Level Pressure anomalies). These relationships with Lifted Index, Precipitable Water and Sea Level Pressure did not exist during the June-September month grouping, most likely due to the prevailing tropical airmasses and higher temperatures during the summer months. This could have an impact on forecasting hail within the state based on seasonal changes.

The different regions of Florida all have unique correlations between atmospheric variables leadings to the occurrence of hail days, discussed in Section 3.5. In Northwest Florida, the climate is such that, in the fall, spring and winter, frontal systems are a regular occurrence which can bring sizeable hail; while during the summer, regular thunderstorms can produce hail from the Gulf of Mexico sea breeze. Additionally, the Central Florida region is prone to more violent, hail producing storms than the other regions during the summer due to the collision of the two sea breeze fronts (whereas Northwest and Northeast Florida only have one sea breeze front).

Objective 3 Discussion

"To suggest better hail forecast methods and extend hail forecast range for Florida, based on a regional and/or seasonal scale, incorporating results from objectives 1 and 2."

Extending hail forecast range in Florida does not seem possible using data from this study. In many cases at day -3, trends toward the increase in one variable (such as Precipitable Water) or decrease in others (Lifted Index) were not present. Usually, there is a trend at day -2 to day -1 and then to day 0 (these trends can be seen in the hail inch size analyses as well as on the composite NCEP/NCAR Reanalysis images themselves). Therefore, predicting a hail event beyond 48 hours (2 days prior to a hail event) would most likely be inaccurate without very high resolution mesoscale models.

Forecasting suggestions can be made using the data, however. While many areas of the country would predict that a lower Lifted Index could translate to larger hail, and higher Precipitable Water may lead to larger hail as well. This is simply not the case in Florida according to the data due to the unique wet and dry seasons experienced in the state. Lower Lifted Index and higher Precipitable Water is mostly associated with small, summer-time hail. Lifted Index in the winter is higher and Precipitable Water is lower compared to the summer/rainy season on hail days, indicating that a low Lifted Index and a high Precipitable Water in Florida does not necessary translate to larger hail. The low Lifted Index during summer is rarely associated with high wind shear, however, which explains the lack of large hail (and high Precipitable Water can be attributed to a prevailing tropical airmass). It is important to take a seasonal approach to hail forecasting when dealing with Florida.

Regionally, there are also several factors to take into account when forecasting hail in Florida. It would be expected that South Florida would receive much more hail during the

summer than any other time of year, as frontal systems do not make their way through the area as often as Northwest Florida, Northeast Florida or even Central Florida. Additionally, South Florida tends not to have as much hail as (and tends to have smaller hail than) other regions, possibly due to higher temperatures and more tropical airmasses causing the freezing level in the atmosphere to move higher (lessening the chance for hail to form or hit the ground before melting). Central Florida, according to raw NOAA archive data, is the most prone to hail days, especially during the summer, when sea breeze fronts from both coasts collide and create stronger summertime thunderstorms than other regions. The different correlations detailed in Section 3.5, as well as the other data described Section 3.1 with regards to data on hail days in the various regions should be taken into consideration when forecasting hail in different regions of Florida.

Chapter Four: Conclusion

Summary

In summary, hail occurrences and hail size in Florida are largely dictated by which season is being observed and which region of Florida is being observed. Overall, the vast majority of hail that falls in Florida is below 2.00" in diameter. Larger hail sizes are observed in the transitional periods between wet and dry season (fall and spring) while smaller hail sizes are associated with summertime sea breeze storms. Additionally, the majority of all hail that occurs in Florida is during the wet season, with more hail occurring in Central Florida than any other region. South Florida received the least hail and smallest hail inch sizes, in part due to the prevailing higher temperatures and tropical airmasses compared to the other regions. With respect to hail size, Vector Wind magnitude was found to increase, at all level studied, as hail size increased.

Several atmospheric variables related to the occurrence of hail days have significant correlations with each other depending on the region and season being observed. Lifted Index is low and Precipitable Water is much higher in the summer during hail events, but are generally lower and higher, respectively, during the summer in Florida, even on non-hail days due to prevailing tropical airmasses and hotter temperatures. Colder temperature anomalies in the mid-levels of the atmosphere (400hPa, 500hPa and 600hPa) tend to occur on hail days in

Florida (except during the summer due to dominant tropical airmasses) while, conversely, warmer Temperatures at 850hPa tend to be associated with hail days (again with the exception of summer). These correlations (among others discussed) and the reasons behind them help to explain why it is important to take into account season and region in Florida when forecasting hail.

Recommendations for Future Study and Limitations

One recommendation for future hail studies in Florida would be to change the month grouping used in this study. The October-January month grouping, in retrospect, may clump together two very different seasons; the end of the wet season and the beginning of the dry season. The results from this month grouping show this. Correlations between different atmospheric variables on hail days seem a mix of the results between the other two month groupings. If the research were to be conducted once again, the "seasonal" split should be based solely on the differences between the wet and dry season. Another alternative would be to focus on the transitional periods between the wet and dry season.

Additionally, researching and analyzing every region of Florida is a large undertaking in one study. Future research should look more in-depth at one specific region, and attempt to further isolate correlations between atmospheric variables on hail days to improve regional forecasting. This should especially be true for South Florida due to its tropical climate.

One major limitation of this study is the analysis of the NCEP/NCAR Reanalysis maps. The maps do not have a large resolution, so assigning the average value of an atmospheric value of a region hundreds of square miles large with a low resolution is not as accurate as it could be. This is complicated further by the low resolution data near the coastline capturing the thermodynamics of the atmosphere over the ocean as well as the thermodynamics of the atmosphere over the land, which is not ideal. This accuracy could change the correlations between atmospheric values on hail days seen in the statistical analysis. However, NCEP/NCAR Reanalysis data were chosen in part due to the data dating back longer than NCEP Climate Forecast System Reanalysis (CFSR) data (which only dates back as far as 1979). Using NCEP/NCAR Reanalysis data as opposed to NCEP/CFSR was also much less time-consuming given the time periods being used. Using NCEP/CFSR data would also be more accurate due to higher resolution models capturing less thermodynamic data over the ocean, lending to a greater amount of data for thermodynamics of the atmosphere over land. A more focused study could rely on other data besides the NCEP/NCAR Reanalysis maps, such as remote sensing data or NCEP/CFSR, to gain knowledge of atmospheric and surface conditions during hail days in Florida.

Another consideration would be to use CAPE instead of Lifted Index, as well as an alternative to Precipitable Water. CAPE is more accurate than Lifted Index, and is considered to be a superior measure by meteorologists as discussed in literature. Although Lifted Index is still used in studies, CAPE would be better and should be considered in any future study. Precipitable Water, while relevant, is also a difficult variable to work with in this study, as it

difficult to know where the moisture is located through the column. For example, the moisture could be spread evenly through the column, or be mostly loaded at one layer in the atmosphere.

Final Thoughts

Researching ways to understand and improve hail forecasting in Florida will not only save millions of dollars for businesses and citizens every year, but may also save citizens from bodily harm, as witnessed in severe weather events such as the “Mayfest“ hailstorm (Jewell and Brimelow 2009). This research can be an aid used to understand and hopefully improve hail forecasting specifically for Florida based on month and region. The data gathered from this research can continue to be added upon by future researchers and can be a valuable asset to hail forecasting and studying hail climatology for the State of Florida. Agriculture, business, weather forecasters, and ordinary citizens can undoubtedly benefit from any improvement in hail forecasting. The methodology employed here can be transferred to other areas or expanded in Florida for future research to realize these potential improvements.

References

Aran, M., J.C. Pena, M. Torà, 2007: Atmospheric circulation patterns associated with hail events in Lleida (Catalonia). *Atmos. Res.*, **100**, 428–438.

Basara, J. B., D. Mitchell, D.R. Cheresnick, B.G. Illston, 2007: An analysis of severe hail swaths in the southern plains of the United States. *Transactions in GIS*, **11**, 531–554.

Brimelow, J.C., G.W. Reuter, 2009: Explicit forecasts of hail occurrence and expected hail size using the GEM–HAILCAST system with a rainfall filter. *Wea. Forecasting*, **24**, 935–945.

Brimelow, J.C., G.W. Reuter, E.R. Poolman, 2002: Modeling maximum hail size in Alberta thunderstorms. *Wea. Forecasting*, **17**, 1048–1062.

Case, J.L., M.M. Wheeler, J. Manobianco, J.W. Weemsand W.P. Roeder, 2005: A 7-yr climatological study of land breezes over the Florida Spaceport. *J. Appl. Meteor.*, **44**, 3403–56.

Cecil, D.J. and C.B Blankenship, 2012: Toward a global climatology of severe hailstorms as estimated by satellite passive microwave imagers. *J. Climate*, **25**, 687–703.

Cheng, L., M. English, R. Wong, 1985: Hailstone Size Distributions and Their Relationship to Storm Thermodynamics. *J. Climate Appl. Meteor*., **24**, 1059–1067.

Crosman, E. T., & J. D. Horel, 2010. Sea and Lake Breezes: A Review of Numerical Studies. *Bound,-Lay. Meteorol.*, **137**, 1–29.

DeRubertis D., 2006. Recent trends in four common stability indices derived from U.S. radiosonde observations. *J.Clim.*, **19(3)**, 309–323.

Earth Systems Research Laboratory, 2010. *NCEP/NCAR Reanalysis 1: Summary*. http://www.esrl.noaa.gov/psd/data/gridded/data.ncep.reanalysis.html. Retrieved 11 Mar 2014.

Farley, R. D., T. Wu, H. D. Orville and M. R. Hjelmfelt, 2004: Numerical simulation of hail formation in the 28 June 1989 Bismarck thunderstorm: Part I. Studies related to hail production. *Atmos. Res.*, **71**, 51–79.

García-Ortega, E., L. López, J.L. Sánchez, 2011: Atmospheric patterns associated with hailstorm days in the EbroValley, Spain. *Atmos. Res.*, **100**, 401–427.

Heinselman, P. L., A.V. Ryzhkov, 2006: Validation of polarimetric hail detection. *Wea. Forecasting*, **21**, 839–850.

Hyvärinen, O. and E. Saltikoff, 2010: Social media as a source of meteorological observations. *Mon. Wea. Rev.*, **138**, 3175–3184.

Jewell, R. and J. Brimelow, 2009: Evaluation of Alberta hail growth model using severe hail proximity soundings from the United States. *Wea. Forecasting*, **24**, 1592–1609.

Kalnay, E., M. Kanamitsu, R. Kistler, W. Collins, D. Deaven, L. Gandin, et al., 1996. The NCEP/NCAR 40-Year Reanalysis Project. *Bull. Amer. Meteor. Soc.*, **77**, 437–470

Kaltenböcka, R., G. Diendorferc, N. Dotzekd, 2009: Evaluation of thunderstorm indices from ECMWF analyses, lightning data and severe storm reports. *Atmos. Res.*, **93**, 381–396.

Leslie, L. M., M. Leplastrier, B.W. Buckley, 2008: Estimating future trends in severe hailstorms over the Sydney Basin: A climate modelling study. *Atmos. Res.*, **87**, 37–51.

Longley, R.W. and C. E. Thompson, 1965: A study of causes of hail *J. Applied Meteor.*, **4**, 69–82.

López, L., E. García-Ortega, J.L. Sánchez, 2005: A short-term forecast model for hail. *Atmos. Res.*, **83**, 176–184.

López, L., J.L. Marcos, J.L. Sánchez, A. Castro, R. Fraile, 2001: CAPE values and hailstorms on northwestern Spain. *Atmos. Res.*, **56**, 147–160.

Manzato, A., 2003: A climatology of instability indices derived from Friuli Venezia Giulia soundings, using three different methods. *Atmos. Res.*, **67–68**, 417–454.

Manzato A., 2012. Hail in Northeast Italy: Climatology and bivariate analysis with the sounding-derived indices. *J.-Appl. Meteor. Climatol.*, **51(3)**, 449–467.

McKnight, T. L., and D. Hess, 2000: *Physical geography: a landscape appreciation 10th Edition*. Prentice Hall, 312 pp.

National Weather Service, 2013: Glossary. Retrieved 10 October 2013.

Nelson, S.P., 1983: The influence of storm flow structure on hail growth. *J. Atmos. Sci.*, **40**, 1965–1983.

Palencia, C., D. Giaiotti, F. Stel, A. Castro, and R. Fraile, 2010: Maximum hailstone size: Relationship with meteorological variables. *Atmos. Res*., **96**, 256–265.

Pflaum, J.C., 1980: Hail formation via microphysical recycling. *J. Atmos. Sci.*, **37**, 160–173.

Scijinks, 2014. Hail Formation. Retrieved April 20th 2014. http://scijinks.nasa.gov/rain

Sánchez, J. L., M.V. Fernández, J.T. Fernández, E. Tuduri, C. Ramis, 2003: Analysis of mesoscale convective systems with hail precipitation. *Atmos. Res.*, **67–68**, 573–588.

Smith, S. R., J. Brolley, J. J. O'Brien, & C. A. Tartaglione, 2007. ENSO's Impact on Regional U.S. Hurricane Activity. *J. Clim.*, **20**, 1404–1414.

Appendices

Table 15: Correlations: February-May Month Grouping (Part 1)

		LI	PW	SLP	T400	T500	T600	T850	VW200	VW300
LI	Pearson Correlation	1	.102	-.037	.634**	.595**	.680**	.472*	.471*	.451*
	Sig. (2-tailed)		.629	.862	.001	.002	.000	.017	.018	.024
	N	25	25	25	25	25	25	25	25	25
PW	Pearson Correlation	.102	1	.011	.632**	.517**	.403*	.390	-.306	-.345
	Sig. (2-tailed)	.629		.959	.001	.008	.046	.054	.137	.091
	N	25	25	25	25	25	25	25	25	25
SLP	Pearson Correlation	-.037	.011	1	-.423*	-.563**	-.571**	-.557**	-.278	-.289
	Sig. (2-tailed)	.862	.959		.035	.003	.003	.004	.179	.160
	N	25	25	25	25	25	25	25	25	25
T400	Pearson Correlation	.634**	.632**	-.423*	1	.961**	.909**	.796**	.199	.162
	Sig. (2-tailed)	.001	.001	.035		.000	.000	.000	.341	.438
	N	25	25	25	25	25	25	25	25	25
T500	Pearson Correlation	.595**	.517**	-.563**	.961**	1	.926**	.821**	.225	.201
	Sig. (2-tailed)	.002	.008	.003	.000		.000	.000	.279	.336
	N	25	25	25	25	25	25	25	25	25
T600	Pearson Correlation	.680**	.403*	-.571**	.909**	.926**	1	.830**	.446*	.428*
	Sig. (2-tailed)	.000	.046	.003	.000	.000		.000	.026	.033
	N	25	25	25	25	25	25	25	25	25
T850	Pearson Correlation	.472*	.390	-.557**	.796**	.821**	.830**	1	.490*	.471*
	Sig. (2-tailed)	.017	.054	.004	.000	.000	.000		.013	.018

	N	25	25	25	25	25	25	25	25	25
	Pearson Correlation	.471*	-.306	-.278	.199	.225	.446*	.490*	1	.976**
VW	Sig. (2-tailed)	.018	.137	.179	.341	.279	.026	.013		.000
200	N	25	25	25	25	25	25	25	25	25
	Pearson Correlation	.451*	-.345	-.289	.162	.201	.428*	.471*	.976**	1
VW	Sig. (2-tailed)	.024	.091	.160	.438	.336	.033	.018	.000	
300	N	25	25	25	25	25	25	25	25	25
	Pearson Correlation	.325	-.280	-.492*	.213	.310	.520**	.607**	.787**	.840**
VW	Sig. (2-tailed)	.113	.176	.013	.307	.132	.008	.001	.000	.000
500	N	25	25	25	25	25	25	25	25	25
	Pearson Correlation	.239	-.237	-.655**	.277	.401*	.547**	.673**	.587**	.633**
VW	Sig. (2-tailed)	.251	.253	.000	.180	.047	.005	.000	.002	.001
700	N	25	25	25	25	25	25	25	25	25
	Pearson Correlation	.323	-.101	-.680**	.401*	.502*	.651**	.688**	.466*	.516**
VW	Sig. (2-tailed)	.115	.630	.000	.047	.011	.000	.000	.019	.008
850	N	25	25	25	25	25	25	25	25	25
	Pearson Correlation	.383	-.102	-.722**	.444*	.527**	.656**	.709**	.546**	.595**
VW	Sig. (2-tailed)	.059	.629	.000	.026	.007	.000	.000	.005	.002
925	N	25	25	25	25	25	25	25	25	25
	Pearson Correlation	.127	-.092	-.553**	.189	.256	.442*	.416*	.471*	.514**
VW	Sig. (2-tailed)	.544	.663	.004	.366	.218	.027	.039	.017	.009
SFC	N	25	25	25	25	25	25	25	25	25

Where LI (Lifted Index), PW (Precipitable Water), SLP (Sea Level Pressure), T400 (Temperature at 400hPa), T500 (Temperature at 500hPa), T600 (Temperature at 600hPa), T850 (Temperature at 850hPa), VW200 (Vector Wind at 200hPa), VW300 (Vector Wind at 300hPa), VW500 (Vector Wind at 500hPa), VW700 (Vector Wind at 700hPa), VW850 (Vector Wind at 850hPa), VW925 (Vector Wind at 925hPa), VWSFC (Vector Wind at Surface)

Table 16: **Correlations: February-May Month Grouping (Part 2)**

		VW500	VW700	VW850	VW925	VWSFC
LI	Pearson Correlation	.325	.239	.323	.383**	.127**
	Sig. (2-tailed)	.113	.251	.115	.059	.544
	N	25	25	25	25	25
PW	Pearson Correlation	-.280	-.237	-.101	-.102**	-.092**
	Sig. (2-tailed)	.176	.253	.630	.629	.663
	N	25	25	25	25	25
SLP	Pearson Correlation	-.492	-.655	-.680	-.722*	-.553**
	Sig. (2-tailed)	.013	.000	.000	.000	.004
	N	25	25	25	25	25
T400	Pearson Correlation	.213**	.277**	.401*	.444	.189**
	Sig. (2-tailed)	.307	.180	.047	.026	.366
	N	25	25	25	25	25
T500	Pearson Correlation	.310**	.401**	.502**	.527**	.256
	Sig. (2-tailed)	.132	.047	.011	.007	.218
	N	25	25	25	25	25
T600	Pearson Correlation	.520**	.547*	.651**	.656**	.442**
	Sig. (2-tailed)	.008	.005	.000	.000	.027
	N	25	25	25	25	25
T850	Pearson Correlation	.607*	.673**	.688**	.709**	.416**
	Sig. (2-tailed)	.001	.000	.000	.000	.039
	N	25	25	25	25	25
VW200	Pearson Correlation	.787*	.587	.466	.546	.471
	Sig. (2-tailed)	.000	.002	.019	.005	.017
	N	25	25	25	25	25

VW300	Pearson Correlation	.840*	.633	.516	.595	.514
	Sig. (2-tailed)	.000	.001	.008	.002	.009
	N	25	25	25	25	25
VW500	Pearson Correlation	1	.894	.838*	.829	.738
	Sig. (2-tailed)		.000	.000	.000	.000
	N	25	25	25	25	25
VW700	Pearson Correlation	.894	1	.955**	.887	.676*
	Sig. (2-tailed)	.000		.000	.000	.000
	N	25	25	25	25	25
VW850	Pearson Correlation	.838	.955	1**	.931*	.720*
	Sig. (2-tailed)	.000	.000		.000	.000
	N	25	25	25	25	25
VW925	Pearson Correlation	.829	.887	.931**	1*	.761**
	Sig. (2-tailed)	.000	.000	.000		.000
	N	25	25	25	25	25
VWSFC	Pearson Correlation	.738	.676	.720**	.761	1
	Sig. (2-tailed)	.000	.000	.000	.000	
	N	25	25	25	25	25

Variables explained in Table 15

Table 17: Correlations: June-September Month Grouping (Part 1)

		LI	PW	SLP	T400	T500	T600	T850	VW200	VW300
LI	Pearson Correlation	1	.189	-.124	-.438	-.238	-.241	-.713**	.158	.188
	Sig. (2-tailed)		.452	.625	.069	.342	.335	.001	.531	.456
	N	18	18	18	18	18	18	18	18	18
PW	Pearson Correlation	.189	1	-.063	.267	.495*	.393	-.029	-.608**	-.603**
	Sig. (2-tailed)	.452		.805	.284	.037	.107	.910	.007	.008
	N	18	18	18	18	18	18	18	18	18

SLP	Pearson Correlation	-.124	-.063	1	.536*	.344	.497*	.326	-.005	-.019
	Sig. (2-tailed)	.625	.805		.022	.162	.036	.187	.985	.941
	N	18	18	18	18	18	18	18	18	18
T400	Pearson Correlation	-.438	.267	.536*	1	.903**	.953**	.804**	-.370	-.379
	Sig. (2-tailed)	.069	.284	.022		.000	.000	.000	.130	.121
	N	18	18	18	18	18	18	18	18	18
T500	Pearson Correlation	-.238	.495*	.344	.903**	1	.939**	.578*	-.600**	-.587*
	Sig. (2-tailed)	.342	.037	.162	.000		.000	.012	.008	.010
	N	18	18	18	18	18	18	18	18	18
T600	Pearson Correlation	-.241	.393	.497*	.953**	.939**	1	.676**	-.386	-.374
	Sig. (2-tailed)	.335	.107	.036	.000	.000		.002	.113	.126
	N	18	18	18	18	18	18	18	18	18
T850	Pearson Correlation	-.713**	-.029	.326	.804**	.578*	.676**	1	-.059	-.071
	Sig. (2-tailed)	.001	.910	.187	.000	.012	.002		.817	.781
	N	18	18	18	18	18	18	18	18	18
VW	Pearson Correlation	.158	-.608**	-.005	-.370	-.600**	-.386	-.059	1	.986**

200	Sig. (2-tailed)	.531	.007	.985	.130	.008	.113	.817		.000
	N	18	18	18	18	18	18	18	18	18
VW300	Pearson Correlation	.188	-.603**	-.019	-.379	-.587*	-.374	-.071	.986**	1
	Sig. (2-tailed)	.456	.008	.941	.121	.010	.126	.781	.000	
	N	18	18	18	18	18	18	18	18	18
VW500	Pearson Correlation	.423	-.471*	-.198	-.683**	-.796**	-.658**	-.412	.900**	.908**
	Sig. (2-tailed)	.080	.049	.430	.002	.000	.003	.090	.000	.000
	N	18	18	18	18	18	18	18	18	18
VW700	Pearson Correlation	.278	-.271	-.172	-.317	-.484*	-.341	-.112	.819**	.801**
	Sig. (2-tailed)	.264	.278	.494	.200	.042	.166	.657	.000	.000
	N	18	18	18	18	18	18	18	18	18
VW850	Pearson Correlation	.119	.130	-.199	-.111	-.188	-.179	.061	.410	.328
	Sig. (2-tailed)	.637	.608	.429	.660	.456	.477	.809	.091	.184
	N	18	18	18	18	18	18	18	18	18
VW925	Pearson Correlation	-.075	.590*	-.221	.056	.196	.067	.066	-.174	-.192
	Sig. (2-tailed)	.768	.010	.378	.824	.435	.792	.794	.491	.446
	N	18	18	18	18	18	18	18	18	18

V	Pearson Correlation	-.580*	-.068	-.007	.249	.214	.193	.439	-.036	-.067
W										
S	Sig. (2-tailed)	.012	.788	.979	.319	.393	.444	.069	.889	.793
F										
C	N	18	18	18	18	18	18	18	18	18

Variables explained in Table 15

Table 18: Correlations: June-September Month Grouping (Part 2)

		VW500	VW700	VW850	VW925	VWSFC
LI	Pearson Correlation	.423	.278	.119	-.075	-.580
	Sig. (2-tailed)	.080	.264	.637	.768	.012
	N	18	18	18	18	18
PW	Pearson Correlation	-.471	-.271	.130	.590	-.068*
	Sig. (2-tailed)	.049	.278	.608	.010	.788
	N	18	18	18	18	18
SLP	Pearson Correlation	-.198	-.172	-.199	-.221*	-.007
	Sig. (2-tailed)	.430	.494	.429	.378	.979
	N	18	18	18	18	18
T400	Pearson Correlation	-.683	-.317	-.111*	.056	.249**
	Sig. (2-tailed)	.002	.200	.660	.824	.319
	N	18	18	18	18	18
T500	Pearson Correlation	-.796	-.484*	-.188	.196**	.214
	Sig. (2-tailed)	.000	.042	.456	.435	.393
	N	18	18	18	18	18
T600	Pearson Correlation	-.658	-.341	-.179*	.067**	.193**
	Sig. (2-tailed)	.003	.166	.477	.792	.444
	N	18	18	18	18	18
T850	Pearson Correlation	-.412**	-.112	.061	.066**	.439*
	Sig. (2-tailed)	.090	.657	.809	.794	.069

	N	18	18	18	18	18
VW200	Pearson Correlation	.900	.819**	.410	-.174	-.036**
	Sig. (2-tailed)	.000	.000	.091	.491	.889
	N	18	18	18	18	18
VW300	Pearson Correlation	.908	.801**	.328	-.192	-.067*
	Sig. (2-tailed)	.000	.000	.184	.446	.793
	N	18	18	18	18	18
VW500	Pearson Correlation	1	.802*	.391	-.111**	-.197**
	Sig. (2-tailed)		.000	.109	.662	.434
	N	18	18	18	18	18
VW700	Pearson Correlation	.802	1	.706	.094	-.195*
	Sig. (2-tailed)	.000		.001	.710	.437
	N	18	18	18	18	18
VW850	Pearson Correlation	.391	.706	1	.583	.038
	Sig. (2-tailed)	.109	.001		.011	.881
	N	18	18	18	18	18
VW925	Pearson Correlation	-.111	.094*	.583	1	.383
	Sig. (2-tailed)	.662	.710	.011		.117
	N	18	18	18	18	18
VWSFC	Pearson Correlation	-.197*	-.195	.038	.383	1
	Sig. (2-tailed)	.434	.437	.881	.117	
	N	18	18	18	18	18

Variables explained in Table 15

Table 19: Correlations: October-January Month Grouping (Part 1)

		LI	PW	SLP	T400	T500	T600	T850	VW200	VW300
LI	Pearson Correlation	1	-.546	-.877**	.301	.512	.400	.095	.760**	.675*
	Sig. (2-tailed)		.053	.000	.317	.074	.176	.758	.003	.011
	N	13	13	13	13	13	13	13	13	13
PW	Pearson Correlation	-.546	1	.421	-.222	-.371	-.541	-.319	-.388	-.269
	Sig. (2-tailed)	.053		.152	.466	.212	.056	.288	.190	.374
	N	13	13	13	13	13	13	13	13	13
	Pearson Correlation	-.877**	.421	1	-.394	-.601*	-.467	-.221	-.715**	-.687**
	Sig. (2-tailed)	.000	.152		.182	.030	.108	.468	.006	.009
	N	13	13	13	13	13	13	13	13	13
T400	Pearson Correlation	.301	-.222	-.394	1	.891**	.854**	.756**	.386	.445
	Sig. (2-tailed)	.317	.466	.182		.000	.000	.003	.193	.128
	N	13	13	13	13	13	13	13	13	13
T500	Pearson Correlation	.512	-.371	-.601*	.891**	1	.899**	.699**	.359	.370
	Sig. (2-tailed)	.074	.212	.030	.000		.000	.008	.229	.214
	N	13	13	13	13	13	13	13	13	13
T600	Pearson Correlation	.400	-.541	-.467	.854**	.899**	1	.672*	.343	.359
	Sig. (2-tailed)	.176	.056	.108	.000	.000		.012	.252	.228
	N	13	13	13	13	13	13	13	13	13
T850	Pearson Correlation	.095	-.319	-.221	.756**	.699**	.672*	1	.197	.265
	Sig. (2-tailed)	.758	.288	.468	.003	.008	.012		.519	.382
	N	13	13	13	13	13	13	13	13	13
VW200	Pearson Correlation	.760**	-.388	-.715**	.386	.359	.343	.197	1	.973**
	Sig. (2-tailed)	.003	.190	.006	.193	.229	.252	.519		.000
	N	13	13	13	13	13	13	13	13	13
VW300	Pearson Correlation	.675*	-.269	-.687**	.445	.370	.359	.265	.973**	1
	Sig. (2-tailed)	.011	.374	.009	.128	.214	.228	.382	.000	

	N	13	13	13	13	13	13	13	13	13
	Pearson Correlation	.838**	-.285	-.841**	.419	.461	.350	.246	.906**	.925**
VW5	Sig. (2-tailed)	.000	.345	.000	.154	.113	.241	.417	.000	.000
00	N	13	13	13	13	13	13	13	13	13
	Pearson Correlation	.886**	-.333	-.863**	.437	.501	.333	.269	.852**	.838**
VW7	Sig. (2-tailed)	.000	.266	.000	.135	.081	.267	.373	.000	.000
00	N	13	13	13	13	13	13	13	13	13
	Pearson Correlation	.718**	-.433	-.726**	.562*	.539	.414	.534	.773**	.781**
VW8	Sig. (2-tailed)	.006	.140	.005	.046	.057	.159	.060	.002	.002
50	N	13	13	13	13	13	13	13	13	13
	Pearson Correlation	.668*	-.612*	-.699**	.524	.561*	.503	.604*	.608*	.626*
VW9	Sig. (2-tailed)	.013	.026	.008	.066	.046	.080	.029	.028	.022
25	N	13	13	13	13	13	13	13	13	13
	Pearson Correlation	.808**	-.486	-.594*	-.011	.178	.038	-.130	.461	.367
VWS	Sig. (2-tailed)	.001	.092	.032	.971	.560	.903	.672	.113	.217
FC	N	13	13	13	13	13	13	13	13	13

Variables explained in Table 15

Table 20: Correlations: October-January Month Grouping (Part 2)

		VW500	VW700	VW850	VW925	VWSFC
	Pearson Correlation	.838	.886	.718**	.668	.808
	Sig. (2-tailed)	.000	.000	.006	.013	.001
LI	N	13	13	13	13	13
	Pearson Correlation	-.285	-.333	-.433	-.612	-.486
	Sig. (2-tailed)	.345	.266	.140	.026	.092
PW	N	13	13	13	13	13
	Pearson Correlation	-.841**	-.863	-.726	-.699	-.594*
	Sig. (2-tailed)	.000	.000	.005	.008	.032
SLP	N	13	13	13	13	13

T400	Pearson Correlation	.419	.437	.562	.524	-.011**
	Sig. (2-tailed)	.154	.135	.046	.066	.971
	N	13	13	13	13	13
T500	Pearson Correlation	.461	.501	.539*	.561**	.178
	Sig. (2-tailed)	.113	.081	.057	.046	.560
	N	13	13	13	13	13
T600	Pearson Correlation	.350	.333	.414	.503**	.038**
	Sig. (2-tailed)	.241	.267	.159	.080	.903
	N	13	13	13	13	13
T850	Pearson Correlation	.246	.269	.534	.604**	-.130**
	Sig. (2-tailed)	.417	.373	.060	.029	.672
	N	13	13	13	13	13
VW200	Pearson Correlation	.906**	.852	.773**	.608	.461
	Sig. (2-tailed)	.000	.000	.002	.028	.113
	N	13	13	13	13	13
VW300	Pearson Correlation	.925*	.838	.781**	.626	.367
	Sig. (2-tailed)	.000	.000	.002	.022	.217
	N	13	13	13	13	13
VW500	Pearson Correlation	1**	.964	.849**	.730	.609
	Sig. (2-tailed)		.000	.000	.005	.027
	N	13	13	13	13	13
VW700	Pearson Correlation	.964**	1	.905**	.778	.709
	Sig. (2-tailed)	.000		.000	.002	.007
	N	13	13	13	13	13
VW850	Pearson Correlation	.849**	.905	1**	.899*	.570
	Sig. (2-tailed)	.000	.000		.000	.042
	N	13	13	13	13	13
VW925	Pearson Correlation	.730*	.778*	.899**	1	.604*
	Sig. (2-tailed)	.005	.002	.000		.029

	N	13	13	13	13	13
	Pearson Correlation	.609**	.709	.570*	.604	1
VWSFC	Sig. (2-tailed)	.027	.007	.042	.029	
	N	13	13	13	13	13

Variables explained in Table 15

Table 21: Correlations: Northwest Region (Part 1)

		LI	PW	SLP	T400	T500	T600	T850	VW200	VW300
LI	Pearson Correlation	1	-.575*	-.720**	-.171	.082	-.176	-.266	.623*	.644**
	Sig. (2-tailed)		.025	.002	.542	.772	.530	.338	.013	.010
	N	15	15	15	15	15	15	15	15	15
PW	Pearson Correlation	-.575*	1	.621*	.170	-.044	-.231	-.409	-.937**	-.949**
	Sig. (2-tailed)	.025		.013	.545	.877	.408	.130	.000	.000
	N	15	15	15	15	15	15	15	15	15
SLP	Pearson Correlation	-.720**	.621*	1	.406	-.122	-.056	.019	-.770**	-.779**
	Sig. (2-tailed)	.002	.013		.133	.664	.844	.946	.001	.001
	N	15	15	15	15	15	15	15	15	15
T400	Pearson Correlation	-.171	.170	.406	1	.627*	.394	.149	-.211	-.230
	Sig. (2-tailed)	.542	.545	.133		.012	.147	.597	.450	.410
	N	15	15	15	15	15	15	15	15	15
T500	Pearson Correlation	.082	-.044	-.122	.627*	1	.637*	.057	.156	.130
	Sig. (2-tailed)	.772	.877	.664	.012		.011	.839	.578	.645
	N	15	15	15	15	15	15	15	15	15
T600	Pearson Correlation	-.176	-.231	-.056	.394	.637*	1	.288	.188	.181
	Sig. (2-tailed)	.530	.408	.844	.147	.011		.297	.503	.519
	N	15	15	15	15	15	15	15	15	15
T850	Pearson Correlation	-.266	-.409	.019	.149	.057	.288	1	.416	.399
	Sig. (2-tailed)	.338	.130	.946	.597	.839	.297		.123	.140
	N	15	15	15	15	15	15	15	15	15

V	Pearson Correlation	.623*	-.937**	-.770**	-.211	.156	.188	.416	1	.996**
W	Sig. (2-tailed)	.013	.000	.001	.450	.578	.503	.123		.000
200	N	15	15	15	15	15	15	15	15	15
V	Pearson Correlation	.644**	-.949**	-.779**	-.230	.130	.181	.399	.996**	1
W	Sig. (2-tailed)	.010	.000	.001	.410	.645	.519	.140	.000	
300	N	15	15	15	15	15	15	15	15	15
V	Pearson Correlation	.737**	-.855**	-.867**	-.312	.116	.132	.283	.931**	.942**
W	Sig. (2-tailed)	.002	.000	.000	.258	.680	.640	.307	.000	.000
500	N	15	15	15	15	15	15	15	15	15
V	Pearson Correlation	.743**	-.799**	-.892**	-.340	.125	.184	.224	.885**	.896**
W	Sig. (2-tailed)	.002	.000	.000	.215	.658	.512	.423	.000	.000
700	N	15	15	15	15	15	15	15	15	15
V	Pearson Correlation	.648**	-.839**	-.792**	-.390	.025	.229	.275	.856**	.874**
W	Sig. (2-tailed)	.009	.000	.000	.151	.929	.412	.322	.000	.000
850	N	15	15	15	15	15	15	15	15	15
V	Pearson Correlation	.513	-.869**	-.746**	-.405	.010	.178	.339	.885**	.895**
W	Sig. (2-tailed)	.051	.000	.001	.134	.971	.526	.217	.000	.000
925	N	15	15	15	15	15	15	15	15	15
V	Pearson Correlation	.511	-.562*	-.733**	-.337	.055	.102	.302	.668**	.658**
WSFC	Sig. (2-tailed)	.051	.029	.002	.220	.845	.717	.273	.007	.008
	N	15	15	15	15	15	15	15	15	15

Variables explained in Table 15

Table 22: Correlations: Northwest Region (Part 2)

		VW500	VW700	VW850	VW925	VWSFC
LI	Pearson Correlation	.737	.743*	.648**	.513	.511
	Sig. (2-tailed)	.002	.002	.009	.051	.051
	N	15	15	15	15	15
PW	Pearson Correlation	-.855*	-.799	-.839*	-.869	-.562
	Sig. (2-tailed)	.000	.000	.000	.000	.029
	N	15	15	15	15	15
SLP	Pearson Correlation	-.867**	-.892*	-.792	-.746	-.733
	Sig. (2-tailed)	.000	.000	.000	.001	.002
	N	15	15	15	15	15
T400	Pearson Correlation	-.312	-.340	-.390	-.405	-.337*
	Sig. (2-tailed)	.258	.215	.151	.134	.220
	N	15	15	15	15	15
T500	Pearson Correlation	.116	.125	.025	.010*	.055
	Sig. (2-tailed)	.680	.658	.929	.971	.845
	N	15	15	15	15	15
T600	Pearson Correlation	.132	.184	.229	.178	.102*
	Sig. (2-tailed)	.640	.512	.412	.526	.717
	N	15	15	15	15	15
T850	Pearson Correlation	.283	.224	.275	.339	.302
	Sig. (2-tailed)	.307	.423	.322	.217	.273
	N	15	15	15	15	15
VW200	Pearson Correlation	.931*	.885**	.856**	.885	.668
	Sig. (2-tailed)	.000	.000	.000	.000	.007
	N	15	15	15	15	15
VW300	Pearson Correlation	.942**	.896**	.874**	.895	.658

	Sig. (2-tailed)	.000	.000	.000	.000	.008
	N	15	15	15	15	15
VW500	Pearson Correlation	1**	.983**	.959**	.923	.822
	Sig. (2-tailed)		.000	.000	.000	.000
	N	15	15	15	15	15
VW700	Pearson Correlation	.983**	1**	.961**	.886	.852
	Sig. (2-tailed)	.000		.000	.000	.000
	N	15	15	15	15	15
VW850	Pearson Correlation	.959**	.961**	1**	.945	.838
	Sig. (2-tailed)	.000	.000		.000	.000
	N	15	15	15	15	15
VW925	Pearson Correlation	.923	.886**	.945**	1	.781
	Sig. (2-tailed)	.000	.000	.000		.001
	N	15	15	15	15	15
VWSFC	Pearson Correlation	.822	.852*	.838**	.781	1
	Sig. (2-tailed)	.000	.000	.000	.001	
	N	15	15	15	15	15

Variables explained in Table 15

Tables 23: Correlations: Northeast Region (Part 1)

		LI	PW	SLP	T400	T500	T600	T850	VW200	VW300
LI	Pearson Correlation	1	-.843**	-.817**	.429	.556*	.427	.743**	.741**	.717**
	Sig. (2-tailed)		.000	.000	.111	.031	.113	.001	.002	.003
	N	15	15	15	15	15	15	15	15	15
PW	Pearson Correlation	-.843**	1	.870**	-.191	-.311	-.219	-.634*	-.683**	-.673**
	Sig. (2-tailed)	.000		.000	.496	.259	.432	.011	.005	.006
	N	15	15	15	15	15	15	15	15	15
SLP	Pearson Correlation	-.817**	.870**	1	-.061	-.279	-.102	-.565*	-.544*	-.520*

P	Sig. (2-tailed)	.000	.000		.829	.313	.717	.028	.036	.047
	N	15	15	15	15	15	15	15	15	15
T400	Pearson Correlation	.429	-.191	-.061	1	.834**	.870**	.720**	.625*	.560*
	Sig. (2-tailed)	.111	.496	.829		.000	.000	.002	.013	.030
	N	15	15	15	15	15	15	15	15	15
T500	Pearson Correlation	.556*	-.311	-.279	.834**	1	.864**	.670**	.457	.383
	Sig. (2-tailed)	.031	.259	.313	.000		.000	.006	.086	.159
	N	15	15	15	15	15	15	15	15	15
T600	Pearson Correlation	.427	-.219	-.102	.870**	.864**	1	.734**	.562*	.498
	Sig. (2-tailed)	.113	.432	.717	.000	.000		.002	.029	.059
	N	15	15	15	15	15	15	15	15	15
T850	Pearson Correlation	.743**	-.634*	-.565*	.720**	.670**	.734**	1	.915**	.882**
	Sig. (2-tailed)	.001	.011	.028	.002	.006	.002		.000	.000
	N	15	15	15	15	15	15	15	15	15
VW200	Pearson Correlation	.741**	-.683**	-.544*	.625*	.457	.562*	.915**	1	.991**
	Sig. (2-tailed)	.002	.005	.036	.013	.086	.029	.000		.000
	N	15	15	15	15	15	15	15	15	15
VW300	Pearson Correlation	.717**	-.673**	-.520*	.560*	.383	.498	.882**	.991**	1
	Sig. (2-tailed)	.003	.006	.047	.030	.159	.059	.000	.000	
	N	15	15	15	15	15	15	15	15	15
VW500	Pearson Correlation	.808**	-.771**	-.667**	.520*	.408	.461	.896**	.976**	.978**
	Sig. (2-tailed)	.000	.001	.007	.047	.131	.083	.000	.000	.000
	N	15	15	15	15	15	15	15	15	15
VW700	Pearson Correlation	.818**	-.790**	-.734**	.453	.363	.389	.861**	.948**	.948**
	Sig. (2-tailed)	.000	.000	.002	.090	.184	.151	.000	.000	.000
	N	15	15	15	15	15	15	15	15	15
VW850	Pearson Correlation	.796**	-.768**	-.760**	.412	.314	.330	.825**	.919**	.912**
	Sig. (2-tailed)	.000	.001	.001	.127	.254	.230	.000	.000	.000
	N	15	15	15	15	15	15	15	15	15

VW925	Pearson Correlation	.865**	-.845**	-.828**	.403	.441	.424	.838**	.862**	.857**
	Sig. (2-tailed)	.000	.000	.000	.136	.100	.115	.000	.000	.000
	N	15	15	15	15	15	15	15	15	15
VWSFC	Pearson Correlation	.786**	-.763**	-.698**	.511	.546*	.576*	.826**	.851**	.833**
	Sig. (2-tailed)	.001	.001	.004	.051	.035	.025	.000	.000	.000
	N	15	15	15	15	15	15	15	15	15

Variables explained in Table 15

Table 24: Correlations: Northeast Region (Part 2)

		VW500	VW700	VW850	VW925	VWSFC
LI	Pearson Correlation	.808	.818**	.796**	.865	.786*
	Sig. (2-tailed)	.000	.000	.000	.000	.001
	N	15	15	15	15	15
PW	Pearson Correlation	-.771**	-.790	-.768**	-.845	-.763
	Sig. (2-tailed)	.001	.000	.001	.000	.001
	N	15	15	15	15	15
SLP	Pearson Correlation	-.667**	-.734**	-.760	-.828	-.698
	Sig. (2-tailed)	.007	.002	.001	.000	.004
	N	15	15	15	15	15
T400	Pearson Correlation	.520	.453	.412	.403	.511**
	Sig. (2-tailed)	.047	.090	.127	.136	.051
	N	15	15	15	15	15
T500	Pearson Correlation	.408*	.363	.314	.441**	.546
	Sig. (2-tailed)	.131	.184	.254	.100	.035
	N	15	15	15	15	15
T600	Pearson Correlation	.461	.389	.330	.424**	.576**
	Sig. (2-tailed)	.083	.151	.230	.115	.025
	N	15	15	15	15	15
T850	Pearson Correlation	.896**	.861*	.825*	.838**	.826**
	Sig. (2-tailed)	.000	.000	.000	.000	.000

	N	15	15	15	15	15
VW200	Pearson Correlation	.976**	.948**	.919*	.862*	.851
	Sig. (2-tailed)	.000	.000	.000	.000	.000
	N	15	15	15	15	15
VW300	Pearson Correlation	.978**	.948**	.912*	.857*	.833
	Sig. (2-tailed)	.000	.000	.000	.000	.000
	N	15	15	15	15	15
VW500	Pearson Correlation	1**	.986**	.958**	.924*	.876
	Sig. (2-tailed)		.000	.000	.000	.000
	N	15	15	15	15	15
VW700	Pearson Correlation	.986**	1**	.986**	.947	.889
	Sig. (2-tailed)	.000		.000	.000	.000
	N	15	15	15	15	15
VW850	Pearson Correlation	.958**	.986**	1**	.943	.877
	Sig. (2-tailed)	.000	.000		.000	.000
	N	15	15	15	15	15
VW925	Pearson Correlation	.924**	.947**	.943**	1	.940
	Sig. (2-tailed)	.000	.000	.000		.000
	N	15	15	15	15	15
VWSFC	Pearson Correlation	.876**	.889**	.877**	.940	1*
	Sig. (2-tailed)	.000	.000	.000	.000	
	N	15	15	15	15	15

Variables explained in Table 15

Table 25: Correlations: Central Region (Part 1)

		LI	PW	SLP	T400	T500	T600	T850	VW200	VW300
LI	Pearson Correlation	1	-.877**	-.620*	.111	.058	-.057	.629*	.866**	.824**
	Sig. (2-tailed)		.000	.024	.719	.851	.852	.021	.000	.001
	N	13	13	13	13	13	13	13	13	13
PW	Pearson Correlation	-.877**	1	.513	-.047	.093	.006	-.553*	-.845**	-.757**
	Sig. (2-tailed)	.000		.073	.879	.762	.984	.050	.000	.003
	N	13	13	13	13	13	13	13	13	13
SLP	Pearson Correlation	-.620*	.513	1	-.211	-.090	.195	-.760**	-.838**	-.897**
	Sig. (2-tailed)	.024	.073		.488	.771	.523	.003	.000	.000
	N	13	13	13	13	13	13	13	13	13
T400	Pearson Correlation	.111	-.047	-.211	1	.947**	.822**	.704**	.047	.045
	Sig. (2-tailed)	.719	.879	.488		.000	.001	.007	.879	.884
	N	13	13	13	13	13	13	13	13	13
T500	Pearson Correlation	.058	.093	-.090	.947**	1	.863**	.588*	-.075	-.065
	Sig. (2-tailed)	.851	.762	.771	.000		.000	.034	.808	.833
	N	13	13	13	13	13	13	13	13	13
	Pearson Correlation	-.057	.006	.195	.822**	.863**	1	.396	-.194	-.250
	Sig. (2-tailed)	.852	.984	.523	.001	.000		.181	.525	.410
	N	13	13	13	13	13	13	13	13	13
T850	Pearson Correlation	.629*	-.553*	-.760**	.704**	.588*	.396	1	.647*	.662*
	Sig. (2-tailed)	.021	.050	.003	.007	.034	.181		.017	.014
	N	13	13	13	13	13	13	13	13	13
VW200	Pearson Correlation	.866**	-.845**	-.838**	.047	-.075	-.194	.647*	1	.985**
	Sig. (2-tailed)	.000	.000	.000	.879	.808	.525	.017		.000
	N	13	13	13	13	13	13	13	13	13
VW300	Pearson Correlation	.824**	-.757**	-.897**	.045	-.065	-.250	.662*	.985**	1

W	Sig. (2-tailed)	.001	.003	.000	.884	.833	.410	.014	.000	
30	N	13	13	13	13	13	13	13	13	13
0										
V	Pearson Correlation	.710**	-.605*	-.945**	.080	-.018	-.271	.673*	.924**	.974**
W	Sig. (2-tailed)	.007	.028	.000	.795	.954	.370	.012	.000	.000
50	N	13	13	13	13	13	13	13	13	13
0										
V	Pearson Correlation	.673*	-.582*	-.967**	.179	.052	-.215	.707**	.902**	.948**
W	Sig. (2-tailed)	.012	.037	.000	.558	.866	.480	.007	.000	.000
70	N	13	13	13	13	13	13	13	13	13
0										
V	Pearson Correlation	.626*	-.542	-.951**	.332	.221	-.038	.794**	.847**	.899**
W	Sig. (2-tailed)	.022	.056	.000	.268	.467	.901	.001	.000	.000
85	N	13	13	13	13	13	13	13	13	13
0										
V	Pearson Correlation	.651*	-.602*	-.854**	.337	.234	.073	.785**	.807**	.841**
W	Sig. (2-tailed)	.016	.030	.000	.261	.441	.812	.001	.001	.000
92	N	13	13	13	13	13	13	13	13	13
5										
V	Pearson Correlation	.765**	-.841**	-.628*	.245	.159	.211	.720**	.805**	.768**
W	Sig. (2-tailed)	.002	.000	.022	.420	.604	.489	.006	.001	.002
S		13	13	13	13	13	13	13	13	13
F	N									
C										

Variables explained in Table 15

Table 26: Correlations: Central Region (Part 2)

		VW500	VW700	VW850	VW925	VWSFC
LI	Pearson Correlation	.710	.673**	.626*	.651	.765
	Sig. (2-tailed)	.007	.012	.022	.016	.002
	N	13	13	13	13	13
PW	Pearson Correlation	-.605**	-.582	-.542	-.602	-.841
	Sig. (2-tailed)	.028	.037	.056	.030	.000
	N	13	13	13	13	13
SLP	Pearson Correlation	-.945*	-.967	-.951	-.854	-.628

	Sig. (2-tailed)	.000	.000	.000	.000	.022
	N	13	13	13	13	13
T400	Pearson Correlation	.080	.179	.332	.337	.245**
	Sig. (2-tailed)	.795	.558	.268	.261	.420
	N	13	13	13	13	13
T500	Pearson Correlation	-.018	.052	.221	.234**	.159
	Sig. (2-tailed)	.954	.866	.467	.441	.604
	N	13	13	13	13	13
T600	Pearson Correlation	-.271	-.215	-.038	.073**	.211**
	Sig. (2-tailed)	.370	.480	.901	.812	.489
	N	13	13	13	13	13
T850	Pearson Correlation	.673*	.707*	.794**	.785**	.720*
	Sig. (2-tailed)	.012	.007	.001	.001	.006
	N	13	13	13	13	13
VW200	Pearson Correlation	.924**	.902**	.847**	.807	.805
	Sig. (2-tailed)	.000	.000	.000	.001	.001
	N	13	13	13	13	13
VW300	Pearson Correlation	.974**	.948**	.899**	.841	.768
	Sig. (2-tailed)	.000	.000	.000	.000	.002
	N	13	13	13	13	13
VW500	Pearson Correlation	1**	.978*	.949**	.867	.695
	Sig. (2-tailed)		.000	.000	.000	.008
	N	13	13	13	13	13
VW700	Pearson Correlation	.978*	1*	.972**	.886	.671
	Sig. (2-tailed)	.000		.000	.000	.012
	N	13	13	13	13	13
VW850	Pearson Correlation	.949*	.972	1**	.938	.723
	Sig. (2-tailed)	.000	.000		.000	.005
	N	13	13	13	13	13

VW925	Pearson Correlation	.867*	.886*	.938**	1	.840
	Sig. (2-tailed)	.000	.000	.000		.000
	N	13	13	13	13	13
VWSFC	Pearson Correlation	.695**	.671**	.723*	.840	1
	Sig. (2-tailed)	.008	.012	.005	.000	
	N	13	13	13	13	13

Variables explained in Table 15

Tables 27: Correlations: South Region (Part 1)

		LI	PW	SLP	T400	T500	T600	T850	VW200	VW300
LI	Pearson Correlation	1	-.400	-.679*	.140	.086	.255	.242	.749**	.774**
	Sig. (2-tailed)		.176	.011	.649	.780	.401	.426	.003	.002
	N	13	13	13	13	13	13	13	13	13
PW	Pearson Correlation	-.400	1	-.027	.619*	.688**	.559*	.188	-.809**	-.795**
	Sig. (2-tailed)	.176		.931	.024	.009	.047	.539	.001	.001
	N	13	13	13	13	13	13	13	13	13
SLP	Pearson Correlation	-.679*	-.027	1	-.624*	-.587*	-.642*	-.551	-.425	-.452
	Sig. (2-tailed)	.011	.931		.023	.035	.018	.051	.147	.121
	N	13	13	13	13	13	13	13	13	13
T400	Pearson Correlation	.140	.619*	-.624*	1	.983**	.955**	.751**	-.123	-.132
	Sig. (2-tailed)	.649	.024	.023		.000	.000	.003	.689	.668
	N	13	13	13	13	13	13	13	13	13
T500	Pearson Correlation	.086	.688**	-.587*	.983**	1	.954**	.698**	-.220	-.222
	Sig. (2-tailed)	.780	.009	.035	.000		.000	.008	.470	.466
	N	13	13	13	13	13	13	13	13	13
T600	Pearson Correlation	.255	.559*	-.642*	.955**	.954**	1	.644*	-.050	-.034
	Sig. (2-tailed)	.401	.047	.018	.000	.000		.018	.872	.913

	N	13	13	13	13	13	13	13	13	13
	Pearson Correlation	.242	.188	-.551	.751**	.698**	.644*	1	.244	.192
T85	Sig. (2-tailed)	.426	.539	.051	.003	.008	.018		.421	.529
0	N	13	13	13	13	13	13	13	13	13
	Pearson Correlation	.749**	-.809**	-.425	-.123	-.220	-.050	.244	1	.992**
VW	Sig. (2-tailed)	.003	.001	.147	.689	.470	.872	.421		.000
200	N	13	13	13	13	13	13	13	13	13
	Pearson Correlation	.774**	-.795**	-.452	-.132	-.222	-.034	.192	.992**	1
VW	Sig. (2-tailed)	.002	.001	.121	.668	.466	.913	.529	.000	
300	N	13	13	13	13	13	13	13	13	13
	Pearson Correlation	.805**	-.765**	-.382	-.188	-.258	-.068	.125	.961**	.977**
VW	Sig. (2-tailed)	.001	.002	.198	.538	.396	.826	.684	.000	.000
500	N	13	13	13	13	13	13	13	13	13
	Pearson Correlation	.751**	-.804**	-.325	-.240	-.325	-.204	.217	.939**	.924**
VW	Sig. (2-tailed)	.003	.001	.279	.430	.279	.503	.476	.000	.000
700	N	13	13	13	13	13	13	13	13	13
	Pearson Correlation	.584*	-.584*	-.302	.100	.007	.154	.422	.725**	.683*
VW	Sig. (2-tailed)	.036	.036	.315	.746	.981	.615	.151	.005	.010
850	N	13	13	13	13	13	13	13	13	13
	Pearson Correlation	.753**	-.316	-.429	.157	.080	.243	.329	.568*	.559*
VW	Sig. (2-tailed)	.003	.293	.144	.609	.795	.424	.272	.043	.047
925	N	13	13	13	13	13	13	13	13	13
	Pearson Correlation	.733**	-.315	-.401	.154	.058	.215	.338	.589*	.570*
VW	Sig. (2-tailed)	.004	.294	.175	.616	.850	.481	.259	.034	.042
SFC	N	13	13	13	13	13	13	13	13	13

Variables explained in Table 15

Table 28: Correlations: South Region (Part 2)

		VW500	VW700	VW850	VW925	VWSFC
LI	Pearson Correlation	.805	.751	.584*	.753	.733
	Sig. (2-tailed)	.001	.003	.036	.003	.004
	N	13	13	13	13	13
PW	Pearson Correlation	-.765	-.804	-.584	-.316*	-.315**
	Sig. (2-tailed)	.002	.001	.036	.293	.294
	N	13	13	13	13	13
SLP	Pearson Correlation	-.382*	-.325	-.302	-.429*	-.401*
	Sig. (2-tailed)	.198	.279	.315	.144	.175
	N	13	13	13	13	13
T400	Pearson Correlation	-.188	-.240*	.100*	.157	.154**
	Sig. (2-tailed)	.538	.430	.746	.609	.616
	N	13	13	13	13	13
T500	Pearson Correlation	-.258	-.325**	.007*	.080**	.058
	Sig. (2-tailed)	.396	.279	.981	.795	.850
	N	13	13	13	13	13
T600	Pearson Correlation	-.068	-.204*	.154*	.243**	.215**
	Sig. (2-tailed)	.826	.503	.615	.424	.481
	N	13	13	13	13	13
T850	Pearson Correlation	.125	.217	.422	.329**	.338**
	Sig. (2-tailed)	.684	.476	.151	.272	.259
	N	13	13	13	13	13
VW200	Pearson Correlation	.961**	.939**	.725	.568	.589
	Sig. (2-tailed)	.000	.000	.005	.043	.034
	N	13	13	13	13	13
VW300	Pearson Correlation	.977**	.924**	.683	.559	.570
	Sig. (2-tailed)	.000	.000	.010	.047	.042

	N	13	13	13	13	13
VW500	Pearson Correlation	1**	.932**	.636	.561	.563
	Sig. (2-tailed)		.000	.020	.046	.045
	N	13	13	13	13	13
VW700	Pearson Correlation	.932**	1**	.683	.580	.604
	Sig. (2-tailed)	.000		.010	.038	.029
	N	13	13	13	13	13
VW850	Pearson Correlation	.636*	.683*	1	.812	.778
	Sig. (2-tailed)	.020	.010		.001	.002
	N	13	13	13	13	13
VW925	Pearson Correlation	.561**	.580	.812	1	.978
	Sig. (2-tailed)	.046	.038	.001		.000
	N	13	13	13	13	13
VWSFC	Pearson Correlation	.563**	.604	.778	.978	1
	Sig. (2-tailed)	.045	.029	.002	.000	
	N	13	13	13	13	13

Variables explained in Table 15